Chirality engineering for carbon nanotube electronics

Dai-Ming Tang[1]*, Ovidiu Cretu[2], Shinsuke Ishihara[1], Yongjia Zheng[3], Keigo Otsuka[3], Rong Xiang[3,4]*, Shigeo Maruyama[3], Hui-Ming Cheng[5,6], Chang Liu[5]*, Dmitri Golberg[1,7]*

1, Research Center for Materials Nanoarchitectonics (MANA), National Institute for Materials Science (NIMS), Tsukuba 305-0044, Japan

2, Center for Basic Research on Materials, National Institute for Materials Science (NIMS), Tsukuba 305-0044, Japan

3, Department of Mechanical Engineering, The University of Tokyo, Tokyo 113-8656, Japan.

4, State Key Laboratory of Fluid Power and Mechatronic Systems, School of Mechanical Engineering, Zhejiang University, Hangzhou, 310027, China

5, Shenyang National Laboratory for Materials Science, Institute of Metal Research, Chinese Academy of Sciences, Shenyang 110016, China

6, Faculty of Materials Science and Energy Engineering/Institute of Technology for Carbon Neutrality, Shenzhen Institute of Advanced Technology, Chinese Academy of Sciences, Shenzhen, 518055, China

7, Centre for Materials Science and School of Chemistry and Physics, Queensland University of Technology (QUT), Brisbane QLD 4000, Australia

*Corresponding authors Emails:

TANG.Daiming@nims.go.jp; xiangrong@zju.edu.cn; cliu@imr.ac.cn; dmitry.golberg@qut.edu.au

Abstract

Carbon nanotubes (CNTs), tubular structures consisting of rolled-up graphene, are promising materials for electronic devices at nanometer and molecular regimes. Fundamentally, electronic properties of CNTs and their junctions are dependent on global and local chiralities, as defined by quantum boundary conditions along circumferential and longitudinal directions. Accordingly, a CNT can behave as a metal, semiconductor, or a quantum dot for building an electronic device. Over the last three decades, great progress has been made in CNT electronics, from building blocks such as resistors and transistors to complex functional devices such as logic and communication devices, thin film and flexible electronics, sensors and intelligent systems, mainly through control over the global chirality distribution of CNTs. In this review article, we summarize approaches to control global and local CNT chiralities by growth and transformation strategies. We then present a perspective regarding new opportunities and challenges for chirality engineering towards raising the performance limit of conventional electronic devices, and development of unconventional CNT quantum electronics. We expect that chirality engineered CNTs will play a key role in ultimately miniaturized transistors, coherent quantum information devices and quantum sensors.

Introduction

As size scaling of Si CMOS approaching the physical limit, great efforts have been devoted to extending the scaling by finding alternative channel materials, integrating more functions, and developing novel electronic devices based on new principles[1,2]. Carbon nanotubes (CNTs) can be visualized through seamlessly rolling up a graphene lattice along a vector, defined as the chirality, into a tubular structure with a diameter of about one nanometer. Electrical properties of CNTs are fundamentally determined by their chiralities, depending on which the CNTs may become metallic or semiconducting[3]. Electrons in nanotubes are ballistically transported over micrometre length due to greatly reduced electron scattering associated with the absence of surface dangling bonds and a quasi-one-dimensional system. The CNTs are chemically stable in air, mechanically flexible, yet tough, due to the strong carbon-carbon covalent bonding. Unique physical properties have made CNTs important candidates for various electronic applications, as a metallic conductor for transparent conducting films (TCFs), and as a semiconductor for efficient nanotransistors and sensors.

Since the pioneering reports on CNT field effect transistors (FETs) 25 years ago[4,5], there have been dramatic progress in CNT electronic devices, due to improvements in growth and processing for highly pure semiconducting nanotubes, and optimization of device configuration and fabrication techniques. Ballistic CNT transistors[6] have been scaled down to 5 nm in gate length[7] and 40 nm in footprint[8], with superior performance compared to silicon counterparts. CNT computers and modern processors have been demonstrated[9,10]. And CNT transistors operated at near-terahertz frequencies[11] have been reported, showing the potential applications in the 6th generation communications. CNTs are promising for flexible and wearable electronic devices because of their high flexibility and strength. By introducing carbon welded joints on the isolated carbon nanotube films, Jiang et al. reported on CNT TCFs with a low sheet resistance close to that of indium tin oxide (ITO)[12]. Sun et al. reported on CNT integrated circuits fabricated on flexible substrates[13]. Zhong et al. optimized the device structure and fabrication process, and prepared integrated circuits based on carbon nanotube films with the oscillation frequency of up to 5.54 GHz[14]. In addition, by coupling electron transport with influences from the environment, ultrahigh sensitivity of CNT based electrochemical and electromechanical systems has been demonstrated for the detection of gas molecules[15], mass[16], force[17], motion[18], charge[19], and so on.

The progress in CNT electronics has been supported by improvements in fabrication of CNTs with desired electrical properties via either direct growth or post-growth separations. Catalysts with stable structure at high temperatures during chemical vapor deposition (CVD) were designed for growing CNTs enriched in semiconducting, metallic, and even specific chiralities[20-26]. Semiconducting CNTs with the purity higher than 99.99 % were successfully separated, enabling the assembled CNT films to be applied as high-performance transistors[27], radio frequency transistors[11] and processors[10]. In this review, distribution of chiralities at macro-scale is defined as "global" chirality. Continued optimization of the global chirality uniformity would be the key for large-scale CNT electronics.

In addition to global chirality, we would like to present the concept of "local" chirality at different segments within an individual CNT. Precise control of the individual and local chiralities for getting a well-defined atomic structure, electronic properties, and junction interfaces, will be indispensable for addressing the electronics with ultimate performance, and would enable unconventional electronics within the quantum regime. In following sections, the concept of global and local chiralities, and their relations with CNT electrical properties will be discussed. The progress of various approaches to engineer CNTs' global and local chirality will be summarized. Then, the progress in CNT electronic devices will be summarized taking transistor-based logic and communication electronics, thin film based-flexible and soft electronics, and sensor-based intelligent systems as examples. After a perspective with an emphasis on new opportunities of local chirality engineering and novel CNT molecular junction devices, challenges in growth, fabrication, characterization, and theory will be discussed.

Main text

1, Chirality and electrical properties of CNTs

1-1 Global chirality of the 1D nanotubes

Electronic band structure of a CNT could be formed by cutting the two-dimensional reciprocal space of graphene along discrete K-lines, as imposed by periodic boundary conditions along the chiral vector. A nanotube will be a metal or a semiconductor depending on whether the K-line crosses the featured Dirac point or not (Fig. 1a-b).[3] Statistically, 1/3 of the nanotubes should be metallic and the remaining 2/3 are semiconducting. For the semiconducting nanotubes, the bandgap (E_g) is inversely

proportional to the diameter (d): $E_g \approx \frac{2\gamma a_{CC}}{d} \sim 0.8eV/d(nm)$, where a_{CC} is the length of the carbon-carbon bonds, and γ is the nearest-neighbour overlap energy[3,28,29].

Near the Fermi level, where electrons for electronic transport are involved, the Fermi velocity could be defined from the band structure as: $\upsilon = \hbar^{-1}\partial\varepsilon/\delta k$. Due to the linear dispersion relationship of the Dirac electrons, CNTs have a large Fermi velocity ~8×10^5 m/s[29], resulting in a high mobility. An important concept in the nanoelectronics is quantum conductance. For the metallic CNTs, there are two sub-bands crossing the Fermi level, resulting in a theoretical conductance of $4G_0$, where $G_0 = \frac{2e^2}{h} \approx 7.75 \times 10^{-5} S$ is the conductance quantum[30]. Experimentally, ballistic transport through metallic nanotubes and semiconducting nanotube channels at ON state has been achieved[6,31,32].

1-2 Local chirality of the nanotube junctions

In the classical model of a CNT, a periodic boundary condition is applied to the longitudinal direction and electron momentum is continuous in the dispersion relation of the band structure. However, to fabricate nanoscale electronic devices, it is necessary to limit the length of the nanotube and to contact it with an electrode. Such a junction is an indispensable part of a device and essentially defines the function.

In conventional semiconductor devices, the basic junction is a p-n junction which is the basic structure of the diodes, light-emitting diodes (LED), photovoltaic (PV) cells and photodetectors. In addition, through combining p-n junctions, transistors could be fabricated to construct logic circuits and the processor of a computer. In CNT electronics, since it is challenging to control doping in the graphitic lattice, instead of conventional p-n junctions, a Schottky junction at the metal-semiconductor interface is the basic junction. Band alignment and the resultant Schottky barrier at the contact not only determines the contact resistance, but also the type of charge carriers in the nanotube channel to be n- or p- type for fabricating complementary metal-oxide semiconductor (CMOS) transistors[32-34].

As the length of a nanotube transistor is scaled down to a few nanometres, in addition to the periodic boundary condition along the circumferential direction, the finite length also imposes quantum confinement effects[29]. Essentially, due to the confinement, the nanotube becomes a quantum dot with the discrete energy levels of which the spacing

is inversely proportional to the junction length: $\Delta E = hv_F/4L_{NT} \approx 1meV/L_{NT}(\mu m)$ (Fig. 1c). Importantly, as the length of the CNT quantum dot is reduced to ~10 nm, the energy level spacings become very large, ~ 0.1 eV, so that CNT quantum dot based quantum electronic devices are expected to function at room temperature[35].

With CNT junctions and quantum dots as building blocks, CNT-based molecular electronic devices have been envisioned theoretically. For example, when a short metallic (5,5) CNT segment is confined between two semiconducting (6,4) CNT segments, instead of a continuous conduction band, isolated localized levels with δ-function-like density of states (DOS) peaks appear in the (5,5) slices, with the energies of the discrete states closely dependent on number of the (5,5) units[36]. On the other hand, with a semiconducting (6,4) segment connected between two metallic (5,5) nanotubes, the device functions as a resonant-tunnelling transistor with the tunnelling current modulated by a gate electrode[37].

1-3 Characterization of CNT chiralities

Global chirality distribution can be measured by using optical spectroscopy[38-40]. In contrast, local chirality of individual CNTs requires high spatial resolution at atomic level. Scanning tunnelling microscopy (STM) has been a powerful tool for determining both the atomic structure and the electronic properties of CNTs, including chirality and van Hove singularities[41]. In addition, distribution of local states of CNT intramolecular junctions has been resolved at atomic resolution[42].

Transmission electron microscopy (TEM) has been at the forefront of CNTs characterization ever since their initial discovery[43]. The most intuitive way to determine the chirality of a CNT is to image it with sufficient resolution and identify positions of each atom. Such observation was reported 13 years after the tubular structures of CNTs were first identified[44,45]. Another option is to operate a microscope in a scanning (STEM) mode, in which a focused probe scans over the sample and forms an image by collecting the detector signal serially, at each probe position. Following the development of aberration-corrected microscopes with high resolution even at a low accelerating voltage, the first STEM images showing single-walled CNT lattice were published in 2010[46,47]. An alternative to imaging in real space is to acquire electron diffraction in the reciprocal space to characterize CNT chirality. This was employed from CNT first observation[43], to prove their helical structure. Over the years, the methods for

determining the chirality of a CNT from its diffraction pattern have been significantly refined[48]. In addition, electron energy-loss spectroscopy (EELS), which measures the energy loss resulting from inelastic interactions, provides rich information about the electronic structure, such as chirality-related van Hove singularities (VHS)[49].

2, Global chirality engineering

Fundamentally, performance of CNT electronic devices depends on quality of the CNT materials, such as purity, wall-number, and diameter, length, defects, and crystallinity, and ultimately the chirality. Ideally, for the large-scale CMOS integrated circuits, it is desired to use well aligned, pure, and densely packed semiconducting single-walled CNTs as the channels[50,51]. On the other hand, for applications in TCFs, purely metallic arm-chair type CNTs are desired, with a suitable density to tune the optical transmittance and the conductivity[52]. For large-scale electronic applications, it is crucial to control the statistical distribution of the CNT chiralities (Fig. 2a), which is defined as the global chirality engineering (Fig. 2b-c) in this review, including organic synthesis[53], "cloning"[54,55], epitaxial growth[22-24,56,57], and post-growth separation[58-61]. The complementary approach of local chirality engineering (Fig. 2d) on the individual nanotubes and segments within nanotubes will be discussed in the next section.

2-1 Chirality-controlled growth

CNTs are typically grown through a CVD process, during which hydrocarbon precursors are decomposed, dissolved, and precipitated under guidance of a growth seed. A lot of research has been devoted to design of the growth seeds, including carbon hemispheres (half-fullerenes), nanotube segments and catalysts with stable structures at high temperatures (Fig. 2b).

Conceptually, a CNT is a hollow cylinder with a cap at each end, which has the same structure as a half-fullerene. It would be desirable to grow the tube part from a half-fullerene molecule which could be synthesized through an organic reaction, at least in principle[53,62]. Itami group demonstrated synthesis of cycloparaphenylenes (CPPs), acene-inserted CPPs, and cyclacenes as the shortest segments and single-unit building blocks of armchair, chiral, and zigzag CNTs, respectively[63]. By using CPPs as growth seeds[63], CNTs with a similar diameter were grown[64]. Fasel and colleagues used (6,6) CNT end caps as seeds to grow (6,6) nanotubes[22]. The precursor of the open-cap molecule ($C_{96}H_{54}$) was designed and synthesized by a multistep organic synthesis

process[65]. Via a cyclodehydrogenation (CDH) process, the precursor was transformed into a short nanotube with a carbon belt connected to the cap. And a nanotube was then continuously grown through epitaxial elongation from the surface-catalyzed decomposition of carbon feedstock gas.

Tour, Smalley, and co-workers proposed and tested the fascinating concept of CNT cloning by activating a metal nanoparticle attached to its tip.[66-68] Yao et al. realized the extension of a CNT by using an open-ended CNT as the growth seed.[54] Liu et al. demonstrated the cloning of CNTs from CNT seeds with predefined chirality, including (7,6), (6,5), and (7,7) types.[54] After a vapour-phase epitaxy (VPE) process, both semiconducting and metallic SWCNTs were significantly elongated to lengths up to tens of micrometres. By optimizing pre-treatment and growth conditions, up to 9 % of the nanotube seeds were elongated successfully, and the yield was improved to 40 % by using quartz as growth substrate[69].

During CVD process, nucleation and growth of a CNT is largely determined by the growth seeds, where the most active catalysts such as iron, cobalt and nickel are in a eutectic, near-liquid phase. In recent years, catalysts with better structural stability and therefore having stable growth interface with CNTs have been intensively investigated for chirality-controlled growth. Bachilo et al. found that (6,5) and (7,5) tubes were predominant, comprising more than 50% of the semiconducting SWCNT grown from the silica-supported Co-Mo catalyst (CoMo CAT) [20]. It was proposed that Mo oxides could stabilize the Co catalyst against aggregation at high temperature for growing CNTs. Yang et al. reported that a single dominating chirality was obtained for CNTs grown from a solid alloy catalyst[23]. Because of the high stability of tungsten-based bimetallic alloy nanocrystals, SWCNTs of a single chirality, (12,6), were produced with an abundance higher than 92 %. Zhang et al. designed Mo_2C and WC catalysts with four-fold and six-fold symmetries[24]. Combining the thermodynamically stable, symmetric interface and the kinetic effects, (2m,m) type CNTs, such as (12,6) and (8,4), were selectively grown to form horizontal arrays.

2-2 Chirality-resolved separation

In addition to control during CNT growth, progress has been made to separate nanotubes by post-synthesis separation[61,70,71]. Various approaches have been developed such as polymer wrapping[72], DNA recognition[59,73], density gradient ultracentrifugation

(DGU)[58] and gel chromatography[60]. Different approaches share the similar general principles of surfactant-assisted dispersion and selective sorting based on molecular interactions (Fig. 2c, e). Compared with direct growth approach, it is easier to scale up the production by separation, however, impurity and structural damage could also be introduced during the processing.

Polymer wrapping has shown selectivity to the diameter and chirality of SWCNTs, so that certain types of SWCNTs could be dispersed and separated using simple sonication and centrifuge equipments[72]. The interaction between the polymer and the CNTs is strongly dependent on the symmetry matching of the backbone structure and electronic interaction (π-bonds), and therefore is sensitive to the slight change of the polymer structure[72]. Nish et al. compared the photoluminescence excitation maps of polymer-SWCNTs with a common part of the repeat unit of poly(9,9-dioctylfluorenyl-2,7-diyl) referred as PFO. Among the four types of polymers, PFO and poly[(9,9-dioctylfluorenyl-2,7-diyl)-alt-co-(1,4-benzo-2,10,3-thiadiazole)], referred as PFO-BT, showed the best separation effects for (8,6) and (10,5) SWCNTs, respectively. Through optimizing the parameters, such as types of polymers, solvent, and temperature, Bao group reported the selectively dispersed s-SWCNTs with high selectivity (>99.7%), high concentration (>0.1 mg/mL), and high yield (>20%)[74,75]. By using high speed shear force instead of sonication to disperse polymer wrapped SWCNTs, Graf et al. realized selective dispersion of nearly pure (6,5) SWCNTs, of which average tube length was as long as 1.82 μm, resulting an ensemble photoluminescence quantum yield (PLQY) of 2.3%[76]. By using the semiconducting nanotubes separated from conjugated polymer-wrapping method as the channel, Brady et al. fabricated CNT array transistors with current density as high as 900 μA/μm, which exceeded that of Si and GaAs FETs[77]. Shi et al. obtained semiconducting nanotubes with the purity as high as 99.99% through polymer wrapping method and reported the aligned CNT array based radio frequency transistors with the operating frequencies up to THz range[11].

Single-stranded DNA (ssDNA) could bind to CNTs through π-stacking, resulting in helical wrapping to assist the dispersion of individual nanotubes[78]. In addition, wrapping of the ssDNA on CNTs was found to be sequence-dependent, so that electrostatics of DNA-CNT hybrid depends on the diameter and electronic properties, therefore CNTs with different electrical properties could be separated by anion exchange chromatography[79]. By improving the ion-exchange chromatography, Zheng

et al. reported separation of single chirality, such as (6,4), (9,1) and (6,5) from CoMoCAT tubes[59]. By choosing suitable DNA sequences, up to 12 types of chiralities of semiconducting SWCNTs have been separated from HiPco nanotubes[73]. In addition to semiconducting nanotubes, Tu et al. realized selective recognition and separation of armchair metallic nanotubes with the chiral indices of (6,6) and (7,7)[73]. The interaction with DNA sequences has been used to assemble the SWCNTs for high performance FETs, with a pitch as small as 10.4 nanometres, an angular deviation smaller than 2° and a yield higher than 95 %[80].

In density gradient ultracentrifugation (DGU), CNTs were dispersed in a solution with selective amphiphilic surfactants and then injected into a fluid medium in a centrifuge tube. Nanotubes with different densities were separated into different layers when a density gradient was generated by a high centripetal force. Initially, separation regarding the diameter, electronic type and bandgap of the CNTs was demonstrated[58]. By developing and improving an orthogonal iterative DGU method, separation of a nearly single-chirality semiconducting (6,5) type from the HiPco SWCNTs with a narrow diameter distribution of 0.01 nm for 99% of the separated nanotubes was achieved[81].

In gel chromatography, selective interaction of CNTs with gel columns was utilized, so that nanotubes with stronger interaction were retained and nanotubes with weaker interaction were passed through[61]. Liu et al. developed a single-surfactant multicolumn gel chromatography method and separated up to 13 different chiralities[60]. Large-scale and industrial-level separation was demonstrated to reach a high concentration of ~1 mg/mL[82]. Tulevski et al. used electrical testing method to characterize ~4000 field-effect transistors with the separated CNTs as the channels[83]. After multiple iterations, 99.9% of the transistors demonstrated semiconducting behaviour. Cao et al. used gel chromatography to separated semiconducting nanotubes with a purity of 99%, and fabricated transistors with the channel consisting of the aligned nanotube arrays[84].

For large-scale applications, both purity and production yield are important. Generally, however, there is a trade-off (Fig. 2e). While in principle, because of the one-to-one relationship between the molecular seeds and the extended nanotubes, it is expected that complete control of the chirality could be reached by the organic synthesis and clone approach, in practice the yield is rather low. On the other hand, near industrial

scale separation of the semiconducting CNTs with high purity has been realized and enabled progresses in nanotube transistors and microprocessors.

3, Local chirality engineering

In addition to global chirality engineering targeting CNT usage in electronic devices based on their assembly, precise control of the local chirality is required for the electronic devices based on individual CNTs and their junctions. Strategies to control the local chirality include chirality changes during growth and mechanical transformation of local structures (Fig. 2d).

3-1 Chirality changes by modulated growth

Just like for any other materials, defects are inevitable during growth of CNTs, leading to random appearance of chirality junctions, as revealed by STM[42], TEM[44], and Raman spectral imaging[85,86]. In addition to the random and spontaneous appearance, some efforts have been made to modulate the growth of CNT by changing growth temperature or applying electrical fields. Yao et al. discovered that by increasing or decreasing growth temperature, diameters of CNTs could be reduced or enlarged, accordingly[87]. By changing the temperature periodically, the chirality of nanotubes was perturbed multiple times, finally leading to the theoretically predicted energetically-preferred near-zigzag chirality[88]. Wang et al. discovered that during growth process, CNTs and catalysts had been charged spontaneously[89]. They developed an electro-renucleation approach to switch the direction of an electric field during synthesis.[90] Due to the different DOS of metallic and semiconducting nanotubes, there was a lower barrier for the metallic nanotubes to renucleate. A metal-to-semiconductor transition was realized to grow aligned semiconducting SWCNTs with residual metallic tubes of less than 0.1 %.

3-2 Chirality transformation by manipulation

Theoretically, two CNTs with different chiral indices could be related by a dislocation in the graphitic lattice. By plastic deformation, the chirality of a nanotube could be transformed to form a CNT molecular junction. In pioneering works of Yakobson and colleagues, theory of the plastic deformation of CNTs has been studied[91-95]. By rotating carbon-carbon bonds, dislocation cores of 5-7 ring pairs could be nucleated and slipped to change the chirality continuously. In addition to the dislocation slip mechanism, Ding et al. proposed the dislocation climb mechanism, where dislocations moved vertically

along the tube axis by removing C_2 dimers[96]. It was predicted that during dislocation slipping, (0,1) type dislocations are energetically preferred so that an armchair type (n,n) nanotube will ultimately transformed into a zigzag (n,0) nanotube[91]. The predicted existence of a possible transformation pattern inspired the explorations for controllable chirality transformations.

Experimentally, Huang et al. applied tension and high temperature from Joule heating by using in situ TEM probing method and observed the surprising superplastic deformation with a tensile strain of 280% and 15-fold reduction in diameter, in contrast to the maximum tensile strain of less than 15% at room temperature[97]. The formation, reconstruction, and healing processes of the defects under the electron beam irradiation and high temperature have been understood in the framework of the dislocation theories[96,98,99]. Cheng et al. further demonstrated that it is possible to shrink the diameters of individual CNTs continuously, uniformly, and flawlessly by electron irradiation at a high temperature[100].

Recently, Tang et al. fabricated suspended CNT transistors and simultaneously monitored the chirality transitions and changes of electronic properties during the in situ TEM manipulation and measurements[101,102]. With measured electronic transport properties as feedback control signal, controlled metal-to-semiconductor transition has been realized. By tracking the chirality changes in 29 consecutive transitions, a transformation pattern towards larger chiral angle was discovered (Fig. 2f). CNT transistors with the channel length as short as ~2.8 nm have been created, and quantum interference has been observed at room temperature.

In contrast to the intensive research in the global chirality engineering and relatively mature techniques, the local chirality engineering approach has just emerged and been addressed just in few experimental reports. Because of the potential to control the chirality with atomic precision and the new opportunities of quantum devices enabled by the nanotube molecular junctions, it is expected that the local chirality engineering should become an active research field.

4, Progress of CNT electronic devices

Fundamentally, all CNT electronic devices are based on the chirality, and are built on the building blocks of resistors, transistors, and sensors (Fig. 3a-b). While the ultimate device performance is determined by the chirality and intrinsic properties of CNTs

which is the focus of the current review, the achievable device performance is strongly dependent on the processing and fabrication procedures. It is crucial to optimize the device geometry and configurations, including the position, length, alignment, density of the nanotubes, the interfaces between the nanotubes and the contact electrodes, oxide dielectric layer and the substrates. Key processing techniques have been developed, including assembly, deposition, printing, transfer and so on, which have been previously reviewed in details[103-107].

As shown in Fig. 3, there is a wide range of CNT electronic devices, which can be mainly categorized into two groups. The first is the "pure" electronic devices that depend on the electron transport, such as nanotransistors (Fig. 3c), microprocessors (Fig. 3d), and amplifiers (Fig. 3e). The other large group is the "functional" devices that couple electronic transport with mechanical, optical, and chemical properties, to form optoelectronic, electro-mechanical and electro-chemical devices, such as transparent electrodes for OLEDs (Fig. 3f), flexible transistors on plastic substrates (Fig. 3g), electronic skins based on flexible pressure sensors (Fig. 3h), and so on, for broad applications ranging from displays, communications, computing, Internet of things and intelligent systems.

4-1 Logic and communication electronics

Modern information society is built on the "chips", consisting of billions of transistors. Semiconducting CNTs have been considered as ideal FET channels because of the nanometer thickness for effective gate control, near ballistic 1D electron transport with a large Fermi velocity for the high current, and small size associated with the small intrinsic capacitance. Modelling at Very-Large-Scale Integrated (VLSI) circuit-level devices revealed that CNT FETs offer 9× energy-delay product (EDP) benefit compared to Si/SiGe FinFET[108].

Transport in CNT FETs is governed by the metal-semiconductor contacts at the source and drain. Depending on the work function, a Schottky junction or near Ohmic contact could be established. Javey et al. used Pd as the electrode material and realized Ohmic contacted p-type ballistic CNT transistors[6,32]. Zhang et al. found that Sc could form Ohmic contact to n-type CNT FETs and fabricated dope-free CMOS[109]. Franklin et al. investigated the scaling properties of the contact resistance with the gate length scaled down to ~15 nm without incurring short-channel effects[110-112]. Cao et al. fabricated end-

bonded contacts by reaction between CNT and the Mo metal to form a carbide interface, and realized size-independent low contact resistance to demonstrate high-performance CNT FETs with sub-10 nm contact length[113]. Qiu et al. fabricated CNT FETs with the gate length as short as 5 nm (Fig. 3c). By using graphene as the contact, a small subthreshold slope of ~73 meV/dec was demonstrated[7]. Around the same period, Cao et al. fabricated CNT FETs with a footprint of 40 nm and demonstrated a higher current compared to Si counterparts[8], demonstrating the potential applications for the ultra-scaled nanotransistors.

For the large-scale applications of CNT FETs in digital electronics, it is necessary to fabricate a device with densely packed, aligned, impurity-free semiconducting CNT arrays. In 2013, Cao et al. reported the full surface coverage of aligned 99% pure semiconducting SWCNT arrays with a high packing density of 500 tubes/μm using the Langmuir–Schaefer method[84]. The current density was more than 120 μA/μm while keeping the on/off ratio at $\sim 1\times10^3$. By improving the alignment and removing the impurities during the assembling process via a floating evaporative self-assembly (FESA), Brady et al. fabricated aligned CNT FETs arrays with the channel length of about 100 nm. The conductance reached 1.7 mS/μm and the saturated on-state current density reached 900 μA/μm, exceeding those numbers for Si FETs. With a packing density of 47 CNTs/μm, the conductance per CNT reached 0.46 G_0 or 35 μS, approaching ballistic transport[77]. High-performance CNT FETs, logic circuits and integrated circuits were fabricated using aligned, high-density semiconducting CNT arrays, with a stage delay of 12.4 ps and the highest maximum oscillating frequency of >8 GHz for the five-stage ring oscillators[114]. Moreover, modern microprocessors built from 14,000 CMOS CNT FETs have been reported (Fig. 3d), based on the fabrication procedure compatible with the current semiconductor industry[10].

Another important application for CNT transistors is high-frequency electronics for wireless communications. One of the crucial devices is radio frequency (RF) transistors operating at high frequency ranges for the analogue components such as low-noise and linear amplifiers. There are two important benchmarks for the RF transistors: the current-gain cutoff frequency (f_T) and the power-gain cutoff frequency (f_{MAX}), defined as the frequencies at which the current and the power gain become unity, respectively. The ultimate frequency of the CNT RF transistors has been predicted to scale to THz range, owing to the near ballistic transport, high Fermi velocity, high mobility, and

small intrinsic capacitance of the nanotube channels[115-117], with the f_T scaling as 130 GHz/L (gate length in μm) in the ballistic limit[116], and as 80 GHz/L for the ideal transistor structure, respectively[115]. CNT for high-performance RF FETs should be aligned arrays with high density, high carrier mobility, high semiconducting purity, and low contact resistance[118].

In 2008, Chaste et al. reported the microwave range operation of top-gated SWCNT transistors with individual nanotubes as the channels. The transconductance was measured to be ~20 μS within the frequency up to 1.6 GHz[119]. Steiner et al. reported SWCNT array transistors through the aligned assembly of separated, semiconducting carbon nanotubes. At a gate length of 100 nm, the intrinsic current and power gain cut-off frequencies were 153 GHz and 30 GHz, respectively[120]. Cao et al. introduced a self-aligned T-shape gate and assembled well-aligned, high-semiconducting-purity, high-density polyfluorene-sorted semiconducting SWCNTs in a RF transistor. Both current-gain cutoff frequency and maximum oscillation frequency greater than 70 GHz were demonstrated. Recently Peng group realized self-assembly of high semiconducting purity, high density, highly aligned SWCNTs by double-dispersion sorting and binary liquid interface-confined self-assembly (BLIS)[11]. With a semiconducting purity up to 99.99%, a packing density of 120 CNTs/μm, and a gate length of 50 nm, the on-state current was 1.92 mA μm^{-1} and the peak transconductance reached 1.40 mS μm^{-1} at a bias of −0.9 V, leading to a high AC performance of a RF transistor. Current-gain and power-gain cutoff frequencies up to 540 and 306 GHz were demonstrated, reaching the near THz range (Fig. 3e).

4-2 Thin film and flexible electronics

CNTs networks are mechanically tough, thermally, and electrically conductive, and chemically stable. Therefore, macroscopic CNT thin films are considered as ideal building blocks for the fabrication of flexible electronic devices such as TCFs and thin film transistors (TFTs).

TCFs are critical for various optoelectronic and display devices, such as photovoltaic cells, light-emitting diodes (LEDs), liquid crystal displays (LCDs), and touch screens for wearable electronics. There is usually a tradeoff between the conductivity and transmittance of thin films. Since SWCNTs are composed of a single graphitic layer and are highly conductive, they are considered ideal for fabricating TCFs with a high

optical transmittance and a low sheet resistance[52]. Theoretically, densely aligned isolated armchair SWCNTs are ideal to construct TCFs with a high optical transmittance and a low sheet resistance. Progress has been made by controlling the bundle size[12], diameter[121] and doping of SWCNTs.

Metallic SWCNTs have much smaller resistance compared to their semiconducting counterparts. Hou et al. synthesized TCFs consisting of enriched metallic SWCNTs (~88%) by controlling the tube diameter and in situ selective oxidation[122]. For the HNO_3 doped SWCNT film, a low sheet resistance of 160 Ω sq^{-1} was measured at 90% transmittance (550 nm). To decrease the contact resistance between crossed SWCNTs, Jiang et al. prepared a network of isolated SWCNTs, in which crossed SWCNTs are welded together by graphitic carbon. It was demonstrated that the carbon-welded joints convert the Schottky contacts between metallic and semiconducting SWCNTs into near-Ohmic ones, which significantly improves the conductivity of the transparent SWCNT network[12]. As a result, an ultra-low sheet resistance of 41 Ω sq^{-1} was achieved at 90% transmittance (550 nm) for the undoped SWCNT films, with uniform and bright luminance from an organic LED demonstrated (Fig. 3f).

TFTs are important for the flat panel displays in smartphones, computers, and TVs. It is desirable to directly grow semiconductor-rich SWCNT networks for the TFTs applications to avoid the damage during the post-growth processing. Yu et al. directly prepared semiconducting SWCNT films using an oxygen-assisted floating catalyst chemical vapor deposition (FCCVD) method, based on the principle that metallic SWCNTs are chemically more reactive than their semiconducting counterparts[123]. The content of semiconducting SWCNTs was estimated to be around 90%, and the fabricated TFTs showed on-off ratios up to ~100. Since the conductivity of the CNT network is determined by the percolation, it is possible to get a macroscopic semiconducting network with a density lower than the percolation threshold. Flexible integrated circuits including a 21-stage ring oscillator and master-slave delay flip-flops were demonstrated[13]. Chen et al. fabricated all-carbon nanotube TFTs[124] (Fig. 3g) which simultaneously possess a high carrier mobility of 33 $cm^2 V^{-1} s^{-1}$ and a high current on/off ratio of $>10^5$, paving the way for low-cost, scalable fabrication of flexible and transparent CNT-based integrated circuits.

4-3 Sensors and intelligent systems

Sensors that detect, measure, and convert a physical or chemical quantity into a signal are crucial in the information driven smart society. CNTs combine several unique properties that make them suitable for the applications in sensors, including the high carrier mobility, high current density, superior mechanical robustness, and chemical stability. Along with the CNT "pure" electronic device discussed in the last two sections, there has been a great progress in CNT "functional" sensors, from an individual sensor to intelligent sensing systems and complex neurological systems.

CNT chemical sensors have been developed for detecting broad ranges of analytes relevant to energy, environment, food, health, and security, including H_2[125], carbon monoxide[126], formaldehyde[127], ethylene[128], biogenic amines[129], proteins[130], antibodies[131], glucose[132], explosives,[133] and toxic chemicals[134]. CNTs have several advantages for the applications in chemical sensors. Firstly, all the atoms of the single-walled CNTs are at the surface and exposed to the environment. Secondly, the diameter of the nanotubes is comparable with the molecules and the electrostatic screening length in the solutions. Therefore, high sensitivity is expected for the CNT sensors. Because of the high sensitivity, inevitable effects, such as O_2/H_2O doping and gradual contamination should be taken into accounts for practical implementation[135]. There are mainly two kinds of CNT chemical sensors. CNT chemiresistors are cheap, and suitable for low-cost applications[128,134,136]. On the other hand, transistors typically have higher sensitivity. Different principles have been proposed for sensing mechanisms of the CNT electrochemical sensors, including the electrostatic gating and modulation of the Schottky barriers[137].

In 2000, Kong et al. reported a chemical sensor based on an individual s-SWCNT transistor[15]. The bottom-gated FET device demonstrated dramatic increase or decrease of electrical resistance in response to NO_2 or NH_3 gas traces (2 ppm-0.1%) at room temperature. The electrical response was explained by a molecular gating effect. The sensitivity of CNT network sensors is strongly dependent on the purity of semiconducting nanotubes. In 2018, Xiao et al. reported the sub-ppm detection limit of H_2, by using high semiconducting purity (>99.9%) solution-derived CNT films as the transistor channel[138]. By designing a specific receptor to functionalize CNT, the selectivity of the targeted detections could be greatly enhanced. In the CNT biosensors, DNA segments could be used to selectively match the targeted biomarkers. Liang et al.

reported on the CNT FET-based biosensors using polymer-sorted high-purity semiconducting CNT films as channel materials. The channel was covered by an ultrathin Y_2O_3 high-κ dielectric layer. With Au nanoparticles as linkers to the probe DNA, a record detection limits as low as 60 aM and 6 particles/mL was demonstrated for the target DNA complementary sequences[139].

Integrated sensing systems that combined the sensing, memory, computing, and communications are under development. Shulaker et al. reported such a system that included four monolithically integrated vertical layers: a top layer of CNT FET gas sensors; a layer of resistive random-access memory (RRAM) cells to store the data; then a layer of CNT logic circuit as decoders for classification; and a Si FET logic layer for computation[140]. By using the principal-component analysis, mixed gases could be classified. In 2023, Fan et al. reported on the monolithic three-dimensional sensing systems consisted of FET sensors and integrated circuits both based on network CNTs at different layers[141]. The upper layer was CNT FET-based hydrogen sensors. The bottom layer was CNT CMOS voltage-controlled oscillator (VCO) interfacing circuits. The information of hydrogen concentration was transformed into the oscillating frequency shift with a sensitivity of 2.75 MHz/ppm.

As mentioned in the previous section, the high carrier mobility combined with the high flexibility of CNTs due to the high tensile strength and low bending stiffness makes them specially promising for the soft, flexible, stretchable, and wearable electronics[103,105]. For a human body, the skin is the largest organ that directly interacts with the world with complex biological, mechanical, and thermal sensing functions[142]. For the soft robot, it is an important goal to mimic the skin's sensory functions[143,144]. Nela et al. fabricated electronic skin consisted of 16×16 arrays of CNT TFTs as a flexible pressure sensor(Fig. 3h)[145]. With a modest operating voltage of 3V, the CNT based artificial skin demonstrated a spatial resolution of 4 mm and a response time of 30 ms which is faster than that of human skin. In addition to static sensors, Wan et al. developed artificial neurological electronic skins based on CNT synaptic transistors[146] to mimic the synaptic behaviors of human skins. Force input was sensed by flexible ferroelectric nanogenerator acting as the peripheral nerves to generate potential pulses that are transmitted to the gates of the CNT TFTs, leading to changes of the drain-source current as the postsynaptic current signal. Various synaptic characteristics have been

demonstrated including the long/short term plasticity, spike amplitude, width, and time related plasticity.

5, Outlook of chirality-engineered CNT electronic devices

Progress in CNT electronics over the last 25 years was the result of improvements in CNT materials and device configurations. Up to now, CNT electronics has been utilizing the classical electronic properties, e.g., semiconducting, or metallic. However, a CNT is not only a metal, or a semiconductor defined by the band structure, but also a unique molecule with the properties distinctly dependent on the local chirality. There are still numerous opportunities to design the molecular structure of CNTs for their applications as quantum devices, for quantum computation, quantum communications and quantum sensors. In this section, we will give a perspective for the CNT electronics with ultimate performance with the complete control over the chirality and properties of CNTs on the global and local levels.

5-1 Ultimate transistors

Future smart society depends on continued and disruptive innovations, such as virtual reality and robotics, which call for more computing power. In this section, we describe a future transistor for the ultimate scaling and performance, including the key components of a transistor: channel, contact, gate, and dielectric layer (Fig. 4a).

Channel: single chirality semiconducting SWCNTs

Semiconducting CNTs have been considered as the ideal channel for nanotransistors. The ultimate challenge is control of the chirality and impurity of the metallic nanotubes. Though up to 99.99% pure semiconducting nanotubes could be separated, the purity is still far behind the desired level of 99.999999%[10]. In addition to the conductance type, the uniformity of the devices depends on the distribution of the chiralities in the semiconducting nanotubes. It is still the greatest challenge to improve the quality of nanotube films to get higher purity of semiconducting nanotubes by global chirality engineering. An alternative approach is the combination of bottom-up growth and top-down transformation to control the chirality for each nanotube.

Contact: metallic nanotube junction

In addition to the channel, the contact is critical for scaling the transistor size to the limit, because of the increased parasitic capacitance and resistance[110], which will

severely affect the operating frequencies of the RF transistors. Previous studies have shown that the end-bonded contact could effectively reduce the contact resistance and enhance the on-current[113]. Furthermore, atomically thin graphene contact was critical to improve the gate controllability for the CNT FETs scaled to 5-nm gate length[7].

For CNTs, due to the 1D electrostatics and screening effects, the electric field distribution is strongly affected by the thickness of the contact[147]. At molecular level, a metallic nanotube junction is potentially the ultimate solution for the contact to reduce parasitic capacitance and to reach ballistic contact limit. The small thickness could contribute to an effective gate control. The covalent bonding between the metallic nanotube lead and the semiconducting channel guarantees effective electrical and thermal conductivity. In addition, the small width of the nanotube reduces the parasitic capacitance to enhance the operating frequency. Our recent work demonstrated that it is possible to fabricate the metallic-semiconducting nanotube junctions as the ultimate contact for the nanotube transistors[102].

Gate and dielectric: van der Waals layers

Currently, state-of-the-art CNT transistors are top gated with a planar shaped metal electrode separated with an oxide insulating layer[7,8]. For Si transistors, the invention of Fin-shaped gate has been one of the keys for improved electrostatic control and continuing scaling. The ideal gate configuration would be the gate-all-around (GAA) for effective gate modulation. Since CNTs have a round tubular cross-section, the GAA FET is a natural selection, as modelled in a recent work[148], where it was predicted that CNT FETs could be scaled down to 5 nm gate-length for a competitive performance and power consumption.

Recent realization of 1D van der Waals heterostructures starting from SWCNTs[149,150] suggests the possibility of an ultimate architecture for GAA-CNT-FETs. These hetero-nanotubes allow to combine materials with distinct electronic properties including the semiconducting nanotube channel, dielectric layer and even metal electrode to form a coaxial FET with each shell to guarantee the atomic level thickness. To reduce the interface trap density in a FET, 1D vdW heterostructures of SWCNTs and surrounding boron nitride nanotubes (BNNTs) may offer the best interface quality, which can be evidenced from the previous studies of two-dimensional semiconductor materials[151]. Near-ideal subthreshold swing with negligible hysteresis may be obtained in such 1D

GAA-CNT-FET. In addition, in principle, it is possible to use the recently discovered van der Waals layered dielectric materials with high dielectric constant for more effective gate control[152]. A metallic-semiconducting-metallic CNT junction with the van der Waals GAA configuration represents the scaling limit of a transistor.

5-2 Quantum transistors

With the length of CNT transistor further reduced, quantum confinement and tunnelling will dominate the electron transport. It is predicted that the physical limit of conventional CMOS FETs will be around 3 nm due to band-to-band tunnelling[153]. While quantum effects are the obstacles for scaling conventional transistors, they can be used to develop quantum transistors, including the single electron transistors (SETs) based on quantum confinement and the tunnelling field-effect transistors (TFETs) based on tunnelling effects.

The working principles of SETs and TFETs are closely related[29,154]. The difference is the coupling strength of the channel with the contact. In the strong coupling limit, in the quantum regime, electrons travel through the channel in a coherent manner, resulting in the interference of incoming, reflected, and transmitted waves. On the other hand, in the weak coupling limit, electrons could tunnel in and out of the channel (island) one-by-one due to the so-called Coulomb blockade. The featured energy levels are closely related to the length of the CNT section. Most previous experiments have been conducted at extremely low temperatures, due to the large length from ~100 nm to ~1 μm[6,31,155-158]. In our recent work, CNT molecular junction transistors with the channel length shorter than 10 nm have been fabricated, and quantum transport such as the Fabry-Pérot oscillations have been observed at room temperature[102], paving the way for practical applications of CNT quantum transistors.

5-3 Quantum sensors

CNT thin film FETs have demonstrated ultra-high sensitivity as gas- and biosensors, thanks to the improvements of the purity of semiconducting nanotubes[138,139,159]. However, under practical conditions, man-made sensors including CNT sensors are still far behind the performance of natural sensors, such as a dog's nose. Currently, the selectivity of CNT FETs depends on the extrinsic decorating metal particles or organic functional groups. Another drawback is that in contrast to the fast response (within several seconds) owing to full exposure of the nanotube surface to environments, the

CNT FET sensors exhibit quite slow recovery (minutes). To further enhance the CNT sensors performance, such as selectivity, response and recover time, quantum principles will be helpful.

As mentioned in the previous section about the CNT quantum transistors operating at room temperature, the most important applications of the quantum transistors will be the quantum sensors (Fig. 4b). It is well known that SETs are extremely sensitive to the local electrical fields and charges, with the sensitivity of a single charge[160]. Conventional SETs are fabricated as quantum dots within semiconductor interfaces with the typical size of ~100 nm. With the proposed CNT molecular junction SETs, it is expected that the operating temperature will increase dramatically and may even approach room temperature. In combination with the extremely small size, it may be not just a dream to use the CNT SETs to map the electromagnetic fields within the brain at ambient conditions.

For the other type of CNT quantum transistors based on the gate modulated tunneling, due to the coherent transport nature, it is expected that the CNT TFETs could be applied as ultra-fast molecule sensors. The local potential could be affected by the absorption of a molecule depending on the interaction of the orbitals. Accordingly, the phase of the electron wave will be modulated, resulting in the shift of the resonance peaks. Real time response to individual molecules could be used as a nanoscale mass spectrometer and to count the molecules in a mixture.

6 Challenges and concluding remarks

We have summarised various progresses of CNT electronics along with improvements in controlling the distribution of the CNT chirality and conductance-type. In addition to global chirality engineering of the overall distribution, we have seen new opportunities of local chirality engineering to fabricate CNT molecular junction devices for the quantum transistors and sensors. However, there are many fundamental and practical challenges with respect to the growth, fabrication, characterization, and theory, towards the dream applications of CNT molecular electronics devices.

6-1 Complete chirality-controlled growth

There has been great progress in the global chirality engineering for getting semiconducting, metallic, and even specific chirality enriched CNTs. Following the laboratory successes, it remains a challenging task to realize chirality-controlled growth

at a large scale. On the other hand, milligram scale separation of semiconducting, metallic, or even single chirality nanotubes have been realized, showing the great potential for industrial scale applications. In contrast to the progress in controlling the chirality distribution, the control of the local chirality of individual CNTs remains largely unexplored. Up to now, there have been only a few reports on the modulated growth of CNT molecular junctions. And no control of the specific chirality for the junctions has been reported.

Since the transport of the CNT SETs and TFETs is sensitive to the atomic structure of the junctions, including the chirality, length, and the interface structures, direct synthesis through the organic reactions is highly appealing because of the possibility of atomically precise design at molecule level. To understand the growth mechanism, especially the chirality transformation mechanism, it is highly desired to observe the growth process of individual CNTs with atomic resolution. In addition, to grow the chirality controlled CNTs and CNT junctions in a predicted manner, it may be necessary to build machine learning model by collecting large amounts of data to relate growth parameters with the resulted chirality and transitions.

6-2 Precise fabrication of molecular junction devices

Currently, CNT electronic devices are either based on individual nanotubes or thin films. To make full use of the chirality-controlled CNT and CNT junctions, it is important to control the position of the junctions and alignment of the devices with a nanometre precision. In addition, it will be a great challenge to fabricate CNT junction devices with the GAA configuration which includes the metallic nanotube junction as the source and the drain, a coaxial shell of high-κ dielectric layer and a metal gate electrode. The possibility of growing h-BN and MoS_2 with high crystallinity on CNTs has been demonstrated, however it remains to be explored to grow other van der Waals layered materials.

A central task for CNT junction devices is formation of the chirality junction in a controlled manner. Our recent work on in situ TEM probing has provided an opportunity to investigate the chirality transformations under high temperature and mechanical stress at the atomic resolution. This revealed a surprising trend for the chiral angle to increase to the armchair type[102]. However, obviously, the in situ manipulation method on individual nanotubes could not be the complete solution for practical

applications. It would be great but not impossible challenge to transfer the in situ fabrication procedure into a microfabrication foundry. And a machine learning model to relate processing parameters to the chirality changes would be very useful.

6-3 Atomic characterization of the transformation mechanism

To tackle the challenges in growth and device fabrication for the CNT molecular junction devices, we have seen several advanced characterizations, especially the in situ TEM. In addition, artificial intelligence (AI) will play critical roles to establish the relations between the growth conditions and processing parameters with the atomic structures, including the chirality and interfaces. However, there are still fundamental limitations and practical challenges for the characterizations of the CNT junction-based structures and devices.

Direct imaging either in TEM or STEM modes suffers from low contrast from the substrate and thermal vibrations of suspended nanotubes. Electron diffraction is less sensitive to the vibrations and is an important technique to determine the CNT chirality. However, due to the reciprocal relationship between real space and diffraction space, it is difficult to collect sharp diffraction patterns from small areas, such as the nanoscale CNT junction devices. The last few years have seen development of several powerful TEM techniques, made possible by new hardware and gains in computing power. One example is 4D-STEM (Fig. 4c), in which a 2D image of the local reciprocal space is recorded for each position of the electron beam[161]. The data can be processed to reconstruct the phase of the object by ptychography[162], which significantly improved the contrast and resolution of DWCNT and SWCNT images[163,164]. In addition, STEM-EELS could give mapping of the electronic states, including bandgap of the junctions.

Finally, the rise in computer power allows for AI being used more and more commonly to automatically process the large amount of data that modern instruments can acquire, which, in the case of CNTs, covers many different fields and techniques[165]. Particularly interesting for the current overview is the use of machine learning to determine the CNT chirality from high resolution images, which can work even in the presence of defects[166].

6-4 Concluding remarks

Chirality engineering is a new paradigm for carbon nanotube electronics. With complete control of the chirality, performance of CNT electronic devices will approach the theoretical limit. More importantly, a local chirality engineering-enabled CNT

molecular junction device is a fundamental shift from the conventional electronic devices that are based on the metallic or semiconducting properties of the nanotubes to the unconventional quantum devices that are based on the quantum confinement and tunnelling transport. Importantly, due to the extremely small size and large energy spacings, the CNT junction devices are expected to be operational at room temperature for the applications, such as brain mapping. There are great challenges for chirality-controlled growth mechanisms and precise device fabrication. We envision that the solutions for the challenges will include advanced in situ TEM characterizations and AI. After three decades, CNT electronics is ready for a leap into the quantum world.

References

1 Bohr, M. T. & Young, I. A. CMOS scaling trends and beyond. *Ieee Micro* **37**, 20-29, doi:10.1109/MM.2017.4241347 (2017).

2 Cavin, R. K., Lugli, P. & Zhirnov, V. V. Science and engineering beyond Moore's law. *P Ieee* **100**, 1720-1749, doi:10.1109/JPROC.2012.2190155 (2012).

3 Saito, R., Fujita, M., Dresselhaus, G. & Dresselhaus, M. S. Electronic structure of chiral graphene tubules. *Appl Phys Lett* **60**, 2204-2206, doi:10.1063/1.107080 (1992).

4 Martel, R., Schmidt, T., Shea, H. R., Hertel, T. & Avouris, P. Single- and multi-wall carbon nanotube field-effect transistors. *Appl Phys Lett* **73**, 2447-2449, doi:doi:http://dx.doi.org/10.1063/1.122477 (1998).

5 Tans, S. J., Verschueren, A. R. M. & Dekker, C. Room-temperature transistor based on a single carbon nanotube. *Nature* **393**, 49-52, doi:10.1038/29954 (1998).

6 Javey, A., Guo, J., Wang, Q., Lundstrom, M. & Dai, H. J. Ballistic carbon nanotube field-effect transistors. *Nature* **424**, 654-657, doi:10.1038/nature01797 (2003).

7 Qiu, C. *et al.* Scaling carbon nanotube complementary transistors to 5-nm gate lengths. *Science* **355**, 271-276, doi:10.1126/science.aaj1628 (2017).

8 Cao, Q., Tersoff, J., Farmer, D. B., Zhu, Y. & Han, S.-J. Carbon nanotube transistors scaled to a 40-nanometer footprint. *Science* **356**, 1369, doi:10.1126/science.aan2476 (2017).

9 Shulaker, M. M. *et al.* Carbon nanotube computer. *Nature* **501**, 526-530, doi:10.1038/nature12502 (2013).

10 Hills, G. *et al.* Modern microprocessor built from complementary carbon nanotube transistors. *Nature* **572**, 595-602, doi:10.1038/s41586-019-1493-8 (2019).

11 Shi, H. *et al.* Radiofrequency transistors based on aligned carbon nanotube arrays. *Nat Electron* **4**, 405-415, doi:10.1038/s41928-021-00594-w (2021).

12 Jiang, S. *et al.* Ultrahigh-performance transparent conductive films of carbon-welded isolated single-wall carbon nanotubes. *Sci Adv* **4**, eaap9264, doi:10.1126/sciadv.aap9264 (2018).

13 Sun, D.-M. *et al.* Flexible high-performance carbon nanotube integrated circuits. *Nat Nanotech* **6**, 156-161, doi:10.1038/nnano.2011.1 (2011).

14 Zhao, C. *et al.* Exploring the performance limit of carbon nanotube network film field-effect transistors for digital integrated circuit applications. *Adv Funct Mater* **29**, 1808574, doi:10.1002/adfm.201808574 (2019).

15 Kong, J. *et al.* Nanotube molecular wires as chemical sensors. *Science* **287**, 622-625, doi:10.1126/science.287.5453.622 (2000).

16 Chaste, J. *et al.* A nanomechanical mass sensor with yoctogram resolution. *Nat Nanotech* **7**, 301-304, doi:10.1038/nnano.2012.42 (2012).

17 Lipomi, D. J. *et al.* Skin-like pressure and strain sensors based on transparent elastic films of carbon nanotubes. *Nat Nanotech* **6**, 788-792, doi:10.1038/nnano.2011.184 (2011).

18 Yamada, T. *et al.* A stretchable carbon nanotube strain sensor for human-motion detection. *Nat Nanotech* **6**, 296-301, doi:10.1038/nnano.2011.36 (2011).

19 Zbydniewska, E. *et al.* Charge blinking statistics of semiconductor nanocrystals revealed by carbon nanotube single charge sensors. *Nano Lett* **15**, 6349-6356, doi:10.1021/acs.nanolett.5b01338 (2015).

20 Bachilo, S. M. *et al.* Narrow (n,m)-distribution of single-walled carbon nanotubes grown using a solid supported catalyst. *J Am Chem Soc* **125**, 11186-11187, doi:10.1021/ja036622c (2003).

21 Harutyunyan, A. R. *et al.* Preferential growth of single-walled carbon nanotubes with metallic conductivity. *Science* **326**, 116-120, doi:10.1126/science.1177599 (2009).

22 Sanchez-Valencia, J. R. *et al.* Controlled synthesis of single-chirality carbon nanotubes. *Nature* **512**, 61-64, doi:10.1038/nature13607 (2014).

23 Yang, F. *et al.* Chirality-specific growth of single-walled carbon nanotubes on solid alloy catalysts. *Nature* **510**, 522-524, doi:10.1038/nature13434

http://www.nature.com/nature/journal/v510/n7506/abs/nature13434.html#supplementary-information (2014).

24 Zhang, S. *et al.* Arrays of horizontal carbon nanotubes of controlled chirality grown using designed catalysts. *Nature* **543**, 234, doi:10.1038/nature21051 (2017).

25 Zhang, S., Tong, L. & Zhang, J. The road to chirality-specific growth of single-walled carbon nanotubes. *National Science Review* **5**, 310-312, doi:10.1093/nsr/nwx080 (2018).

26 Yang, F. *et al.* Chirality pure carbon nanotubes: growth, sorting, and characterization. *Chem Rev* **120**, 2693-2758, doi:10.1021/acs.chemrev.9b00835 (2020).

27 Liu, C. *et al.* Complementary transistors based on aligned semiconducting carbon nanotube arrays. *ACS Nano* **16**, 21482-21490, doi:10.1021/acsnano.2c10007 (2022).

28 White, C. T. & Mintmire, J. W. Density of states reflects diameter in nanotubes. *Nature* **394**, 29-30, doi:10.1038/27801 (1998).

29 Charlier, J.-C., Blase, X. & Roche, S. Electronic and transport properties of nanotubes. *Rev Mod Phys* **79**, 677-732, doi:10.1103/RevModPhys.79.677 (2007).

30 White, C. T. & Todorov, T. N. Carbon nanotubes as long ballistic conductors. *Nature* **393**, 240-242, doi:10.1038/30420 (1998).

31 Liang, W. *et al.* Fabry - Perot interference in a nanotube electron waveguide. *Nature* **411**, 665-669, doi:10.1038/35079517 (2001).

32 Mann, D., Javey, A., Kong, J., Wang, Q. & Dai, H. Ballistic transport in metallic nanotubes with reliable Pd Ohmic contacts. *Nano Lett* **3**, 1541-1544, doi:10.1021/nl034700o (2003).

33 Heinze, S., Radosavljević, M., Tersoff, J. & Avouris, P. Unexpected scaling of the performance of carbon nanotube Schottky-barrier transistors. *Phys Rev B* **68**, 235418, doi:10.1103/PhysRevB.68.235418 (2003).

34 Chen, Z., Appenzeller, J., Knoch, J., Lin, Y.-m. & Avouris, P. The role of metal−nanotube contact in the performance of carbon nanotube field-effect transistors. *Nano Lett* **5**, 1497-1502, doi:10.1021/nl0508624 (2005).

35 Rochefort, A., Salahub, D. R. & Avouris, P. Effects of finite length on the electronic structure of carbon nanotubes. *J Phys Chem B* **103**, 641-646, doi:10.1021/jp983725m (1999).

36 Chico, L., López Sancho, M. P. & Muñoz, M. C. Carbon-nanotube-based quantum dot. *Phys Rev Lett* **81**, 1278-1281, doi:10.1103/PhysRevLett.81.1278 (1998).

37 Hyldgaard, P. & Lundqvist, B. I. Robust nanosized transistor effect in fullerene-tube heterostructure. *Solid State Commun* **116**, 569-573, doi:10.1016/S0038-1098(00)00377-X (2000).

38 Jorio, A. *et al.* Structural (n,m) determination of isolated single-wall carbon nanotubes by resonant Raman scattering. *Phys Rev Lett* **86**, 1118-1121, doi:10.1103/PhysRevLett.86.1118 (2001).

39 Bachilo, S. M. *et al.* Structure-assigned optical spectra of single-walled carbon nanotubes. *Science* **298**, 2361-2366, doi:10.1126/science.1078727 (2002).

40 Liu, K. *et al.* An atlas of carbon nanotube optical transitions. *Nat Nanotech* **7**, 325-329, doi:10.1038/nnano.2012.52 (2012).

41 Wilder, J. W. G., Venema, L. C., Rinzler, A. G., Smalley, R. E. & Dekker, C. Electronic structure of atomically resolved carbon nanotubes. *Nature* **391**, 59-62, doi:10.1038/34139 (1998).

42 Ouyang, M., Huang, J.-L., Cheung, C. L. & Lieber, C. M. Atomically resolved single-walled carbon nanotube intramolecular junctions. *Science* **291**, 97-100, doi:10.1126/science.291.5501.97 (2001).

43 Iijima, S. Helical microtubules of graphitic carbon. *Nature* **354**, 56-58, doi:10.1038/354056a0 (1991).

44 Hashimoto, A., Suenaga, K., Gloter, A., Urita, K. & Iijima, S. Direct evidence for atomic defects in graphene layers. *Nature* **430**, 870-873, doi:10.1038/nature02817 (2004).

45 Meyer, R. R. *et al.* A composite method for the determination of the chirality of single walled carbon nanotubes. *Journal of Microscopy* **212**, 152-157, doi:10.1046/j.1365-2818.2003.01240.x (2003).

46 Krivanek, O. L. *et al.* Gentle STEM: ADF imaging and EELS at low primary energies. *Ultramicroscopy* **110**, 935-945, doi:10.1016/j.ultramic.2010.02.007 (2010).

47 Sasaki, T. *et al.* Performance of low-voltage STEM/TEM with delta corrector and cold field emission gun. *J Electron Microsc* **59**, S7-S13, doi:10.1093/jmicro/dfq027 (2010).

48 Qin, L.-C. Electron diffraction from carbon nanotubes. *Rep Prog Phys* **69**, 2761, doi:10.1088/0034-4885/69/10/R02 (2006).

49 Sato, Y., Terauchi, M., Mukai, M., Kaneyama, T. & Adachi, K. High energy-resolution electron energy-loss spectroscopy study of the dielectric properties of bulk and nanoparticle LaB6 in the near-infrared region. *Ultramicroscopy* **111**, 1381-1387, doi:10.1016/j.ultramic.2011.05.003 (2011).

50 Franklin, A. D. The road to carbon nanotube transistors. *Nature* **498**, 443, doi:10.1038/498443a (2013).

51 Peng, L.-M., Zhang, Z. & Qiu, C. Carbon nanotube digital electronics. *Nature Electronics* **2**, 499-505, doi:10.1038/s41928-019-0330-2 (2019).

52 Ilatovskii, D. A., Gilshtein, E. P., Glukhova, O. E. & Nasibulin, A. G. Transparent conducting films based on carbon nanotubes: rational design toward the theoretical Limit. *Advanced Science* **9**, 2201673, doi:10.1002/advs.202201673 (2022).

53 Segawa, Y., Yagi, A., Matsui, K. & Itami, K. Design and synthesis of carbon nanotube segments. *Angew Chem Int Edit* **55**, 5136-5158, doi:10.1002/anie.201508384 (2016).

54 Yao, Y., Feng, C., Zhang, J. & Liu, Z. "Cloning" of single-walled carbon nanotubes via open-end growth mechanism. *Nano Lett* **9**, 1673-1677, doi:10.1021/nl900207v (2009).

55 Liu, J. *et al.* Chirality-controlled synthesis of single-wall carbon nanotubes using vapour-phase epitaxy. *Nat Commun* **3**, 1199, doi:10.1038/ncomms2205 (2012).

56 Reich, S., Li, L. & Robertson, J. Control the chirality of carbon nanotubes by epitaxial growth. *Chem Phys Lett* **421**, 469-472, doi:10.1016/j.cplett.2006.01.110 (2006).

57 Zhang, F., Hou, P.-X., Liu, C. & Cheng, H.-M. Epitaxial growth of single-wall carbon nanotubes. *Carbon* **102**, 181-197, doi:10.1016/j.carbon.2016.02.029 (2016).

58 Arnold, M. S., Green, A. A., Hulvat, J. F., Stupp, S. I. & Hersam, M. C. Sorting carbon nanotubes by electronic structure using density differentiation. *Nat Nanotech* **1**, 60-65, doi:10.1038/nnano.2006.52 (2006).

59 Zheng, M. & Semke, E. D. Enrichment of single chirality carbon nanotubes. *J Am Chem Soc* **129**, 6084-6085, doi:10.1021/ja071577k (2007).

60 Liu, H., Nishide, D., Tanaka, T. & Kataura, H. Large-scale single-chirality separation of single-wall carbon nanotubes by simple gel chromatography. *Nat Commun* **2**, 309, doi:10.1038/ncomms1313 (2011).

61 Wei, X. *et al.* Recent advances in structure separation of single-wall carbon nanotubes and their application in optics, electronics, and optoelectronics. *Advanced Science* **9**, 2200054, doi:10.1002/advs.202200054 (2022).

62 Segawa, Y., Ito, H. & Itami, K. Structurally uniform and atomically precise carbon nanostructures. *Nat Rev Mater* **1**, 15002, doi:10.1038/natrevmats.2015.2 (2016).

63 Omachi, H., Segawa, Y. & Itami, K. Synthesis of cycloparaphenylenes and related carbon nanorings: a step toward the controlled synthesis of carbon nanotubes. *Accounts of Chemical Research* **45**, 1378-1389, doi:10.1021/ar300055x (2012).

64 Omachi, H., Nakayama, T., Takahashi, E., Segawa, Y. & Itami, K. Initiation of carbon nanotube growth by well-defined carbon nanorings. *Nature Chemistry* **5**, 572-576, doi:10.1038/nchem.1655 (2013).
65 Rim, K. T. *et al.* Forming aromatic hemispheres on transition-metal surfaces. *Angew Chem Int Edit* **46**, 7891-7895, doi:10.1002/anie.200701117 (2007).
66 Wang, Y. *et al.* Continued growth of single-walled carbon nanotubes. *Nano Lett* **5**, 997-1002, doi:10.1021/nl047851f (2005).
67 Smalley, R. E. *et al.* Single wall carbon nanotube amplification: en route to a type-specific growth mechanism. *J Am Chem Soc* **128**, 15824-15829, doi:10.1021/ja065767r (2006).
68 Ren, Z. Cloning carbon. *Nat Nanotech* **2**, 17-18, doi:10.1038/nnano.2006.192 (2007).
69 Liu, B., Wu, F., Gui, H., Zheng, M. & Zhou, C. Chirality-controlled synthesis and applications of single-wall carbon nanotubes. *ACS Nano* **11**, 31-53, doi:10.1021/acsnano.6b06900 (2017).
70 Gaviria Rojas, W. A. & Hersam, M. C. Chirality-enriched carbon nanotubes for next-generation computing. *Adv Mater* **32**, 1905654, doi:10.1002/adma.201905654 (2020).
71 Srimani, T. *et al.* Comprehensive study on high purity semiconducting carbon nanotube extraction. *Advanced Electronic Materials* **8**, 2101377, doi:10.1002/aelm.202101377 (2022).
72 Nish, A., Hwang, J.-Y., Doig, J. & Nicholas, R. J. Highly selective dispersion of single-walled carbon nanotubes using aromatic polymers. *Nat Nanotech* **2**, 640-646, doi:10.1038/nnano.2007.290 (2007).
73 Tu, X., Manohar, S., Jagota, A. & Zheng, M. DNA sequence motifs for structure-specific recognition and separation of carbon nanotubes. *Nature* **460**, 250-253, doi:10.1038/nature08116 (2009).
74 Lee, H. W. *et al.* Selective dispersion of high purity semiconducting single-walled carbon nanotubes with regioregular poly(3-alkylthiophene)s. *Nat Commun* **2**, 541, doi:10.1038/ncomms1545 (2011).
75 Lei, T., Pochorovski, I. & Bao, Z. Separation of semiconducting carbon nanotubes for flexible and stretchable electronics using polymer removable method. *Accounts of Chemical Research* **50**, 1096-1104, doi:10.1021/acs.accounts.7b00062 (2017).
76 Graf, A. *et al.* Large scale, selective dispersion of long single-walled carbon nanotubes with high photoluminescence quantum yield by shear force mixing. *Carbon* **105**, 593-599, doi:10.1016/j.carbon.2016.05.002 (2016).
77 Brady, G. J. *et al.* Quasi-ballistic carbon nanotube array transistors with current density exceeding Si and GaAs. *Sci Adv* **2**, doi:10.1126/sciadv.1601240 (2016).
78 Zheng, M. *et al.* DNA-assisted dispersion and separation of carbon nanotubes. *Nat Mater* **2**, 338-342, doi:10.1038/nmat877 (2003).
79 Zheng, M. *et al.* Structure-based carbon nanotube sorting by sequence-dependent DNA assembly. *Science* **302**, 1545-1548, doi:10.1126/science.1091911 (2003).
80 Zhao, M. *et al.* DNA-directed nanofabrication of high-performance carbon nanotube field-effect transistors. *Science* **368**, 878, doi:10.1126/science.aaz7435 (2020).
81 Green, A. A. & Hersam, M. C. Nearly single-chirality single-walled carbon nanotubes produced via orthogonal iterative density gradient ultracentrifugation. *Adv Mater* **23**, 2185-2190, doi:10.1002/adma.201100034 (2011).
82 Yang, D. *et al.* Preparing high-concentration individualized carbon nanotubes for industrial separation of multiple single-chirality species. *Nat Commun* **14**, 2491, doi:10.1038/s41467-023-38133-0 (2023).
83 Tulevski, G. S., Franklin, A. D. & Afzali, A. High purity isolation and quantification of semiconducting carbon nanotubes via column chromatography. *ACS Nano* **7**, 2971-2976, doi:10.1021/nn400053k (2013).

84 Cao, Q. *et al.* Arrays of single-walled carbon nanotubes with full surface coverage for high-performance electronics. *Nat Nanotech* **8**, 180-186, doi:10.1038/nnano.2012.257 (2013).
85 Doorn, S. K. *et al.* Raman spectral imaging of a carbon nanotube intramolecular junction. *Phys Rev Lett* **94**, 016802, doi:10.1103/PhysRevLett.94.016802 (2005).
86 Anderson, N., Hartschuh, A. & Novotny, L. Chirality changes in carbon nanotubes studied with near-field Raman spectroscopy. *Nano Lett* **7**, 577-582, doi:10.1021/nl0622496 (2007).
87 Yao, Y. *et al.* Temperature-mediated growth of single-walled carbon-nanotube intramolecular junctions. *Nat Mater* **6**, 283, doi:10.1038/nmat1865 (2007).
88 Zhao, Q., Xu, Z., Hu, Y., Ding, F. & Zhang, J. Chemical vapor deposition synthesis of near-zigzag single-walled carbon nanotubes with stable tube-catalyst interface. *Sci Adv* **2**, e1501729, doi:10.1126/sciadv.1501729 (2016).
89 Wang, J. *et al.* Observation of charge generation and transfer during CVD growth of carbon nanotubes. *Nano Lett* **16**, 4102-4109, doi:10.1021/acs.nanolett.6b00841 (2016).
90 Wang, J. *et al.* Growing highly pure semiconducting carbon nanotubes by electrotwisting the helicity. *Nat Catal* **1**, 326, doi:10.1038/s41929-018-0057-x (2018).
91 Yakobson, B. I. Mechanical relaxation and "intramolecular plasticity" in carbon nanotubes. *Appl Phys Lett* **72**, 918-920, doi:10.1063/1.120873 (1998).
92 Buongiorno Nardelli, M., Yakobson, B. I. & Bernholc, J. Mechanism of strain release in carbon nanotubes. *Phys Rev B* **57**, R4277-R4280, doi:10.1103/PhysRevB.57.R4277 (1998).
93 Nardelli, M. B., Yakobson, B. I. & Bernholc, J. Brittle and ductile behavior in carbon nanotubes. *Phys Rev Lett* **81**, 4656-4659, doi:10.1103/PhysRevLett.81.4656 (1998).
94 Samsonidze, G. G., Samsonidze, G. G. & Yakobson, B. I. Kinetic theory of symmetry-dependent strength in carbon nanotubes. *Phys Rev Lett* **88**, 065501, doi:10.1103/PhysRevLett.88.065501 (2002).
95 Dumitrica, T., Hua, M. & Yakobson, B. I. Symmetry-, time-, and temperature-dependent strength of carbon nanotubes. *Proc Natl Acad Sci USA* **103**, 6105-6109, doi:10.1073/pnas.0600945103 (2006).
96 Ding, F., Jiao, K., Wu, M. & Yakobson, B. I. Pseudoclimb and dislocation dynamics in superplastic nanotubes. *Phys Rev Lett* **98**, 075503, doi:10.1103/PhysRevLett.98.075503 (2007).
97 Huang, J. Y. *et al.* Superplastic carbon nanotubes. *Nature* **439**, 281-281, doi:10.1038/439281a (2006).
98 Ding, F., Jiao, K., Lin, Y. & Yakobson, B. I. How evaporating carbon nanotubes retain their perfection? *Nano Lett* **7**, 681-684, doi:10.1021/nl0627543 (2007).
99 Huang, J. Y., Ding, F. & Yakobson, B. I. Vacancy-hole and vacancy-tube migration in multiwall carbon nanotubes. *Phys Rev B* **78**, 155436, doi:10.1103/PhysRevB.78.155436 (2008).
100 Cheng, Y., Li, P., Zhang, Q. & Wang, M.-S. Top-down fabrication of small carbon nanotubes. *Nanoscale Horizons*, doi:10.1039/C9NH00285E (2019).
101 Tang, D.-M. *et al.* Chirality transitions and transport properties of individual few-walled carbon nanotubes as revealed by in situ TEM probing. *Ultramicroscopy* **194**, 108-116, doi:https://doi.org/10.1016/j.ultramic.2018.07.012 (2018).
102 Tang, D.-M. *et al.* Semiconductor nanochannels in metallic carbon nanotubes by thermomechanical chirality alteration. *Science* **374**, 1616-1620, doi:10.1126/science.abi8884 (2021).

103 Park, S., Vosguerichian, M. & Bao, Z. A review of fabrication and applications of carbon nanotube film-based flexible electronics. *Nanoscale* **5**, 1727-1752, doi:10.1039/C3NR33560G (2013).

104 Chen, K. *et al.* Printed Carbon Nanotube Electronics and Sensor Systems. *Adv Mater* **28**, 4397-4414, doi:10.1002/adma.201504958 (2016).

105 Koo, J. H., Song, J.-K. & Kim, D.-H. Solution-processed thin films of semiconducting carbon nanotubes and their application to soft electronics. *Nanotechnology* **30**, 132001, doi:10.1088/1361-6528/aafbbe (2019).

106 Qiu, S. *et al.* Solution-processing of high-purity semiconducting single-walled carbon nanotubes for electronics devices. *Adv Mater* **31**, 1800750, doi:10.1002/adma.201800750 (2019).

107 Si, J., Xu, L., Zhu, M., Zhang, Z. & Peng, L.-M. Advances in high-performance carbon-nanotube thin-film electronics. *Advanced Electronic Materials* **5**, 1900122, doi:10.1002/aelm.201900122 (2019).

108 Hills, G. *et al.* Understanding energy efficiency benefits of carbon nanotube field-effect transistors for digital VLSI. *IEEE Transactions on Nanotechnology* **17**, 1259-1269, doi:10.1109/TNANO.2018.2871841 (2018).

109 Zhang, Z. *et al.* Doping-free fabrication of carbon nanotube based ballistic CMOS devices and circuits. *Nano Lett* **7**, 3603-3607, doi:10.1021/nl0717107 (2007).

110 Franklin, A. D., Farmer, D. B. & Haensch, W. Defining and overcoming the contact resistance challenge in scaled carbon nanotube transistors. *ACS Nano* **8**, 7333-7339, doi:10.1021/nn5024363 (2014).

111 Franklin, A. D. *et al.* Sub-10 nm Carbon Nanotube Transistor. *Nano Lett* **12**, 758-762, doi:10.1021/nl203701g (2012).

112 Franklin, A. D. & Chen, Z. Length scaling of carbon nanotube transistors. *Nat Nanotech* **5**, 858, doi:10.1038/nnano.2010.220 (2010).

113 Cao, Q. *et al.* End-bonded contacts for carbon nanotube transistors with low, size-independent resistance. *Science* **350**, 68, doi:10.1126/science.aac8006 (2015).

114 Liu, L. *et al.* Aligned, high-density semiconducting carbon nanotube arrays for high-performance electronics. *Science* **368**, 850, doi:10.1126/science.aba5980 (2020).

115 Burke, P. J. AC performance of nanoelectronics: towards a ballistic THz nanotube transistor. *Solid State Electron* **48**, 1981-1986, doi:10.1016/j.sse.2004.05.044 (2004).

116 Hasan, S., Salahuddin, S., Vaidyanathan, M. & Alam, M. A. High-frequency performance projections for ballistic carbon-nanotube transistors. *IEEE Transactions on Nanotechnology* **5**, 14-22, doi:10.1109/TNANO.2005.858594 (2006).

117 Jing, G., Hasan, S., Javey, A., Bosman, G. & Lundstrom, M. Assessment of high-frequency performance potential of carbon nanotube transistors. *IEEE Transactions on Nanotechnology* **4**, 715-721, doi:10.1109/TNANO.2005.858601 (2005).

118 Rutherglen, C., Jain, D. & Burke, P. Nanotube electronics for radiofrequency applications. *Nat Nanotech* **4**, 811-819, doi:10.1038/nnano.2009.355 (2009).

119 Chaste, J. *et al.* Single Carbon Nanotube Transistor at GHz Frequency. *Nano Lett* **8**, 525-528, doi:10.1021/nl0727361 (2008).

120 Steiner, M. *et al.* High-frequency performance of scaled carbon nanotube array field-effect transistors. *Appl Phys Lett* **101**, 053123, doi:10.1063/1.4742325 (2012).

121 Zhang, Q. *et al.* Large-diameter carbon nanotube transparent conductor overcoming performance–yield tradeoff. *Adv Funct Mater* **32**, 2103397, doi:10.1002/adfm.202103397 (2022).

122 Hou, P.-X. *et al.* Preparation of metallic single-wall carbon nanotubes by selective etching. *ACS Nano* **8**, 7156-7162, doi:10.1021/nn502120k (2014).

123 Yu, B. *et al.* Synthesis of large diameter semiconducting single-walled carbon nanotubes by oxygen-assisted floating catalyst chemical vapor deposition. *J Am Chem Soc* **133**, 5232-5235, doi:10.1021/ja2008278 (2011).
124 Chen, Y.-Y. *et al.* High-throughput fabrication of flexible and transparent all-carbon nanotube electronics. *Advanced Science* **5**, 1700965, doi:10.1002/advs.201700965 (2018).
125 Ganzhorn, M. *et al.* Hydrogen sensing with diameter- and chirality-sorted carbon nanotubes. *ACS Nano* **5**, 1670-1676, doi:10.1021/nn101992g (2011).
126 Savagatrup, S. *et al.* Bio-inspired carbon monoxide sensors with voltage-activated sensitivity. *Angew Chem Int Edit* **56**, 14066-14070, doi:10.1002/anie.201707491 (2017).
127 Ishihara, S., Labuta, J., Nakanishi, T., Tanaka, T. & Kataura, H. Amperometric detection of sub-ppm formaldehyde using single-walled carbon nanotubes and hydroxylamines: a referenced chemiresistive system. *ACS Sensors* **2**, 1405-1409, doi:10.1021/acssensors.7b00591 (2017).
128 Ishihara, S. *et al.* Cascade reaction-based chemiresistive array for ethylene sensing. *ACS Sensors* **5**, 1405-1410, doi:10.1021/acssensors.0c00194 (2020).
129 Liu, S. F., Petty, A. R., Sazama, G. T. & Swager, T. M. Single-walled carbon nanotube/metalloporphyrin composites for the chemiresistive detection of amines and meat spoilage. *Angew Chem Int Edit* **54**, 6554-6557, doi:10.1002/anie.201501434 (2015).
130 Star, A., Gabriel, J.-C. P., Bradley, K. & Grüner, G. Electronic detection of specific protein binding using nanotube FET devices. *Nano Lett* **3**, 459-463, doi:10.1021/nl0340172 (2003).
131 Chen, R. J. *et al.* Noncovalent functionalization of carbon nanotubes for highly specific electronic biosensors. *Proc Natl Acad Sci USA* **100**, 4984-4989, doi:10.1073/pnas.0837064100 (2003).
132 Besteman, K., Lee, J.-O., Wiertz, F. G. M., Heering, H. A. & Dekker, C. Enzyme-coated carbon nanotubes as single-molecule biosensors. *Nano Lett* **3**, 727-730, doi:10.1021/nl034139u (2003).
133 Roberts, M. E., LeMieux, M. C. & Bao, Z. Sorted and aligned single-walled carbon nanotube networks for transistor-based aqueous chemical sensors. *ACS Nano* **3**, 3287-3293, doi:10.1021/nn900808b (2009).
134 Ishihara, S., Azzarelli, J. M., Krikorian, M. & Swager, T. M. Ultratrace detection of toxic chemicals: triggered disassembly of supramolecular nanotube wrappers. *J Am Chem Soc* **138**, 8221-8227, doi:10.1021/jacs.6b03869 (2016).
135 Collins, P. G., Bradley, K., Ishigami, M. & Zettl, A. Extreme oxygen sensitivity of electronic properties of carbon nanotubes. *Science* **287**, 1801-1804, doi:10.1126/science.287.5459.1801 (2000).
136 Ishihara, S. *et al.* Metallic versus semiconducting SWCNT chemiresistors: a case for separated SWCNTs wrapped by a metallosupramolecular polymer. *ACS Applied Materials & Interfaces* **9**, 38062-38067, doi:10.1021/acsami.7b12992 (2017).
137 Heller, I. *et al.* Identifying the mechanism of biosensing with carbon nanotube transistors. *Nano Lett* **8**, 591-595, doi:10.1021/nl072996i (2008).
138 Xiao, M. *et al.* Batch fabrication of ultrasensitive carbon nanotube hydrogen sensors with sub-ppm detection limit. *ACS Sensors* **3**, 749-756, doi:10.1021/acssensors.8b00006 (2018).
139 Liang, Y. *et al.* Wafer-scale uniform carbon nanotube transistors for ultrasensitive and label-free detection of disease biomarkers. *ACS Nano* **14**, 8866-8874, doi:10.1021/acsnano.0c03523 (2020).

140 Shulaker, M. M. *et al.* Three-dimensional integration of nanotechnologies for computing and data storage on a single chip. *Nature* **547**, 74, doi:10.1038/nature22994 (2017).
141 Fan, C. *et al.* Monolithic three-dimensional integration of carbon nanotube circuits and sensors for smart sensing chips. *ACS Nano* **17**, 10987-10995, doi:10.1021/acsnano.3c03190 (2023).
142 Liu, Y., Pharr, M. & Salvatore, G. A. Lab-on-kkin: a review of flexible and stretchable electronics for wearable health monitoring. *ACS Nano* **11**, 9614-9635, doi:10.1021/acsnano.7b04898 (2017).
143 Amjadi, M., Kyung, K.-U., Park, I. & Sitti, M. Stretchable, skin-mountable, and wearable strain sensors and their potential applications: a review. *Adv Funct Mater* **26**, 1678-1698, doi:10.1002/adfm.201504755 (2016).
144 Wang, X. *et al.* Recent progress in electronic skin. *Advanced Science* **2**, 1500169, doi:10.1002/advs.201500169 (2015).
145 Nela, L., Tang, J., Cao, Q., Tulevski, G. & Han, S.-J. Large-Area High-Performance Flexible Pressure Sensor with Carbon Nanotube Active Matrix for Electronic Skin. *Nano Lett* **18**, 2054-2059, doi:10.1021/acs.nanolett.8b00063 (2018).
146 Wan, H. *et al.* Flexible carbon nanotube synaptic transistor for neurological electronic skin applications. *ACS Nano* **14**, 10402-10412, doi:10.1021/acsnano.0c04259 (2020).
147 Heinze, S. *et al.* Carbon nanotubes as Schottky barrier transistors. *Phys Rev Lett* **89**, 106801, doi:10.1103/PhysRevLett.89.106801 (2002).
148 Xu, L. *et al.* Can carbon nanotube transistors be scaled down to the sub-5 nm gate length? *ACS Applied Materials & Interfaces* **13**, 31957-31967, doi:10.1021/acsami.1c05229 (2021).
149 Xiang, R. *et al.* One-dimensional van der Waals heterostructures. *Science* **367**, 537, doi:10.1126/science.aaz2570 (2020).
150 Zheng, Y. *et al.* One-dimensional van der Waals heterostructures: Growth mechanism and handedness correlation revealed by nondestructive TEM. *Proc Natl Acad Sci USA* **118**, e2107295118, doi:10.1073/pnas.2107295118 (2021).
151 Dean, C. R. *et al.* Boron nitride substrates for high-quality graphene electronics. *Nat Nanotech* **5**, 722-726, doi:10.1038/nnano.2010.172 (2010).
152 Zhang, C. *et al.* Single-crystalline van der Waals layered dielectric with high dielectric constant. *Nat Mater* **22**, 832-837, doi:10.1038/s41563-023-01502-7 (2023).
153 Iwai, H. in *16th International Workshop on Junction Technology (IWJT).* (2016).
154 Laird, E. A. *et al.* Quantum transport in carbon nanotubes. *Rev Mod Phys* **87**, 703-764, doi:10.1103/RevModPhys.87.703 (2015).
155 Kane, C., Balents, L. & Fisher, M. P. A. Coulomb interactions and mesoscopic effects in carbon nanotubes. *Phys Rev Lett* **79**, 5086-5089, doi:10.1103/PhysRevLett.79.5086 (1997).
156 Bockrath, M. *et al.* Resonant electron scattering by defects in single-walled carbon nanotubes. *Science* **291**, 283-285, doi:10.1126/science.291.5502.283 (2001).
157 Park, J. *et al.* Coulomb blockade and the Kondo effect in single-atom transistors. *Nature* **417**, 722-725, doi:10.1038/nature00791 (2002).
158 Jarillo-Herrero, P., Sapmaz, S., Dekker, C., Kouwenhoven, L. P. & van der Zant, H. S. J. Electron-hole symmetry in a semiconducting carbon nanotube quantum dot. *Nature* **429**, 389-392, doi:10.1038/nature02568 (2004).
159 Schroeder, V., Savagatrup, S., He, M., Lin, S. & Swager, T. M. Carbon nanotube chemical sensors. *Chem Rev* **119**, 599-663, doi:10.1021/acs.chemrev.8b00340 (2019).
160 Degen, C. L., Reinhard, F. & Cappellaro, P. Quantum sensing. *Rev Mod Phys* **89**, 035002, doi:10.1103/RevModPhys.89.035002 (2017).

161 Ophus, C. Four-dimensional scanning transmission electron microscopy (4D-STEM): from scanning nanodiffraction to ptychography and beyond. *Microsc Microanal* **25**, 563-582, doi:10.1017/S1431927619000497 (2019).
162 Nellist, P. D., McCallum, B. C. & Rodenburg, J. M. Resolution beyond the 'information limit' in transmission electron microscopy. *Nature* **374**, 630-632, doi:10.1038/374630a0 (1995).
163 Yang, H. *et al.* Simultaneous atomic-resolution electron ptychography and Z-contrast imaging of light and heavy elements in complex nanostructures. *Nat Commun* **7**, 12532, doi:10.1038/ncomms12532 (2016).
164 Sagawa, R. *et al.* Low dose imaging by STEM ptychography using pixelated STEM detector. *Microsc Microanal* **24**, 198-199, doi:10.1017/S1431927618001484 (2018).
165 Vivanco-Benavides, L. E., Martínez-González, C. L., Mercado-Zúñiga, C. & Torres-Torres, C. Machine learning and materials informatics approaches in the analysis of physical properties of carbon nanotubes: A review. *Comp Mater Sci* **201**, 110939, doi:10.1016/j.commatsci.2021.110939 (2022).
166 Förster, G. D. *et al.* A deep learning approach for determining the chiral indices of carbon nanotubes from high-resolution transmission electron microscopy images. *Carbon* **169**, 465-474, doi:10.1016/j.carbon.2020.06.086 (2020).

Highlighted references

3 Saito, R., Fujita, M., Dresselhaus, G. & Dresselhaus, M. S. Electronic structure of chiral graphene tubules. *Appl Phys Lett* **60**, 2204-2206, doi:10.1063/1.107080 (1992).

Theoretical work on the chirality-dependent electronic structure of CNTs that predicted 1/3 of the CNTs to be metallic and 2/3 to be semiconductor.

10 Hills, G. *et al.* Modern microprocessor built from complementary carbon nanotube transistors. *Nature* **572**, 595-602, doi:10.1038/s41586-019-1493-8 (2019).

First demonstration of modern microprocessors fabricated from CNT transistors, showing the possibility of CNTs for the large-scale applications.

11 Shi, H. *et al.* Radiofrequency transistors based on aligned carbon nanotube arrays. *Nat Electron* **4**, 405-415, doi:10.1038/s41928-021-00594-w (2021).

First report on the radiofrequency CNT transistors with the maximum and cut-off frequencies in the THz range (540 and 306 GHz, respectively), showing the potentials of CNT electronics in next-generation wireless communications.

20 Bachilo, S. M. *et al.* Narrow (n,m)-distribution of single-walled carbon nanotubes grown using a solid supported catalyst. *J Am Chem Soc* **125**, 11186-11187, doi:10.1021/ja036622c (2003).

Pioneering work on chirality enriched CNTs from stable catalysts at high temperatures.

31 Liang, W. *et al.* Fabry - Perot interference in a nanotube electron waveguide. *Nature* **411**, 665-669, doi:10.1038/35079517 (2001).

Observation of quantum coherent transport of electron waves through the CNT waveguide to form an interference oscillation of the transmittance and conductance.

36 Chico, L., López Sancho, M. P. & Muñoz, M. C. Carbon-nanotube-based quantum dot. *Phys Rev Lett* **81**, 1278-1281, doi:10.1103/PhysRevLett.81.1278 (1998).

Theoretical investigations on the structure and electronic properties of CNT based quantum dots by introducing pentagon-heptagon defects to form short CNT junctions.

38 Jorio, A. *et al.* Structural (n,m) determination of isolated single-wall carbon nanotubes by resonant Raman scattering. *Phys Rev Lett* **86**, 1118-1121 (2001).

Experimental demonstration that even for isolated CNTs, it is possible to determine the diameter and chirality by measuring the radial breathing mode (RBM) frequency using the resonant confocal micro-Raman spectroscopy

41 Wilder, J. W. G., Venema, L. C., Rinzler, A. G., Smalley, R. E. & Dekker, C. Electronic structure of atomically resolved carbon nanotubes. *Nature* **391**, 59-62, doi:10.1038/34139 (1998).

The atomic structure, chirality, and electronic structure of CNTs was characterized by using the scanning tunning microscopy (STM).

58 Arnold, M. S., Green, A. A., Hulvat, J. F., Stupp, S. I. & Hersam, M. C. Sorting carbon nanotubes by electronic structure using density differentiation. *Nat Nanotech* **1**, 60-65, doi:10.1038/nnano.2006.52 (2006).

Successfully sorted CNTs by diameter, bandgap and electronic type by based on the subtle differences in their buoyant densities through the density gradient ultracentrifugation method.

60 Liu, H., Nishide, D., Tanaka, T. & Kataura, H. Large-scale single-chirality separation of single-wall carbon nanotubes by simple gel chromatography. *Nat Commun* **2**, 309, doi:10.1038/ncomms1313 (2011).

Up to 13 different chiral species of CNTs were separated through a single surfactant multicolumn gel chromatography method, showing the potential for industrial scale application of the chirality separated CNTs.

79 Zheng, M. *et al.* Structure-based carbon nanotube sorting by sequence-dependent DNA assembly. *Science* **302**, 1545-1548, doi:10.1126/science.1091911 (2003).

Discovery of the sequence-dependent wrapping CNTs by single-stranded DNA (ssDNA) for the chirality-sorted separation.

87 Yao, Y. *et al.* Temperature-mediated growth of single-walled carbon-nanotube intramolecular junctions. *Nat Mater* **6**, 283, doi:10.1038/nmat1865 (2007).

Experimental demonstration for the growth of CNT molecular junctions by modulating the growth temperature.

90 Wang, J. *et al.* Growing highly pure semiconducting carbon nanotubes by electrotwisting the helicity. *Nat Catal* **1**, 326, doi:10.1038/s41929-018-0057-x (2018).

Discovery of the effects of switching electrical fields leading to the metal-to-semiconductor transition during the growth of CNTs.

91 Yakobson, B. I. Mechanical relaxation and "intramolecular plasticity" in carbon nanotubes. *Appl Phys Lett* **72**, 918-920, doi:10.1063/1.120873 (1998).

Pioneering theoretical work on the mechanism of plastic deformation of CNTs, including the nucleation and sliding of dislocations.

96 Ding, F., Jiao, K., Wu, M. & Yakobson, B. I. Pseudoclimb and dislocation dynamics in superplastic nanotubes. *Phys Rev Lett* **98**, 075503, doi:10.1103/PhysRevLett.98.075503 (2007).

Important theoretical discussions on the dislocation dynamics during the plastic deformation of CNTs, including the dislocation climbing mechanism.

97 Huang, J. Y. *et al.* Superplastic carbon nanotubes. *Nature* **439**, 281-281, doi:10.1038/439281a (2006).

Pioneer in situ TEM observation on the superplastic deformation of CNTs under tensile stress and high temperature.

102 Tang, D.-M. *et al.* Semiconductor nanochannels in metallic carbon nanotubes by thermomechanical chirality alteration. *Science* **374**, 1616-1620, doi:10.1126/science.abi8884 (2021).

Experimental demonstration of feedback-controlled metal-to-semiconductor transition by chirality transformation. CNT transistors with the channel length as short as 2.8 nm were fabricated, showing quantum transport at room temperature.

166 Förster, G. D. *et al.* A deep learning approach for determining the chiral indices of carbon nanotubes from high-resolution transmission electron microscopy images. *Carbon* **169**, 465-474, doi:10.1016/j.carbon.2020.06.086 (2020).

First application of deep learning method to determine the CNT chirality from TEM images.

Acknowledgements

We thank Dr. Don N Futaba and Dr. Guohai Chen (National Institute of Advanced Industrial Science and Technology, Japan) for inspiring discussions. D.M.T. discloses support from JSPS Kakenhi [grant number JP25820336, JP 20K05281, JP 23H01796], JST-FOREST Program [grant number JPMJFR223T, Japan], WPI-MANA "Challenging Research Program (CRP)", and NIMS "Support system for curiosity-driven research". R.X. discloses support from Ministry of Science and Technology of China [grant number 2023YFE0101300] and Zhejiang province [grant number 2022R01001]. H.M.C. discloses support from National Natural Science Foundation of China [grant number 52188101]. C.L. acknowledges support from Ministry of Science and Technology of China [Grant 2022YFA1203302], the National Natural Science Foundation of China [Grants 52130209, 52188101], Liaoning Revitalization Talents Program [XLYC2002037]. D.G. discloses support from Australian Research Council Laureate Fellowship [grant number FL160100089].

Author contributions

D.M.T. led the collaborative work. All authors contributed to the discussions, drafted, and revised on the manuscript.

Competing interests

The authors declare no competing interests.

Key points box

- The electrical properties of CNTs are determined by the chirality along circumferential direction to be metallic or semiconducting, and by the confinement imposed along longitudinal direction to be a quantum dot.
- For the large-scale applications of CNT electronics, approaches have been developed to control the global chirality distribution, including direct growth for defect-free nanotubes and post-growth separation for industrial applications.
- For fabricating CNT molecular junction-based electronic devices, modulated growth and chirality transformation techniques have been explored, however this development is still in its early stage.
- The progress in controlling the global chirality distribution has led to advancements in CNT electronics ranging from transistors, amplifiers, microprocessors, to transparent electrodes, flexible transistors, and electronic skins.
- Complete control of chirality would enable the conventional CNT electronics to approach the performance limit, and create new opportunities for the emerging quantum devices.

Display items

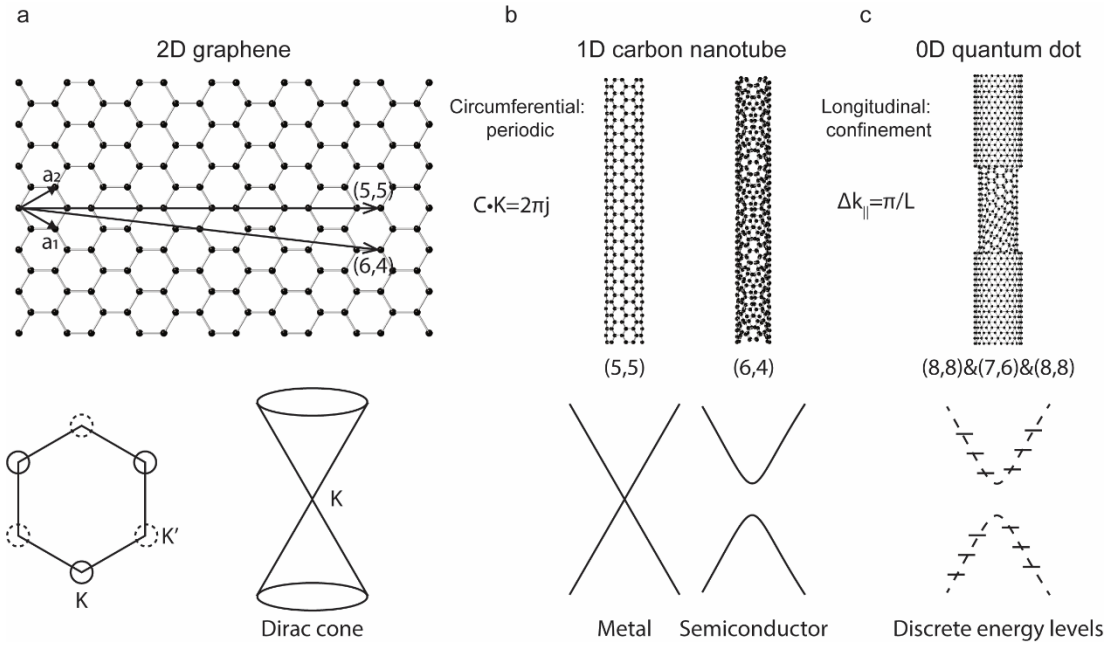

Figure 1. Chirality and the electronic properties of carbon nanotubes. (a) Lattice, Brillouin zone and Dirac cone at one of the K points of 2D graphene. (b) Atomic structure and dispersion relationship of a metallic (5,5) and a semiconducting (6,4) carbon nanotube. (c) Atomic structure and discrete energy levels of a carbon nanotube quantum dot confined within a nanotube junction.

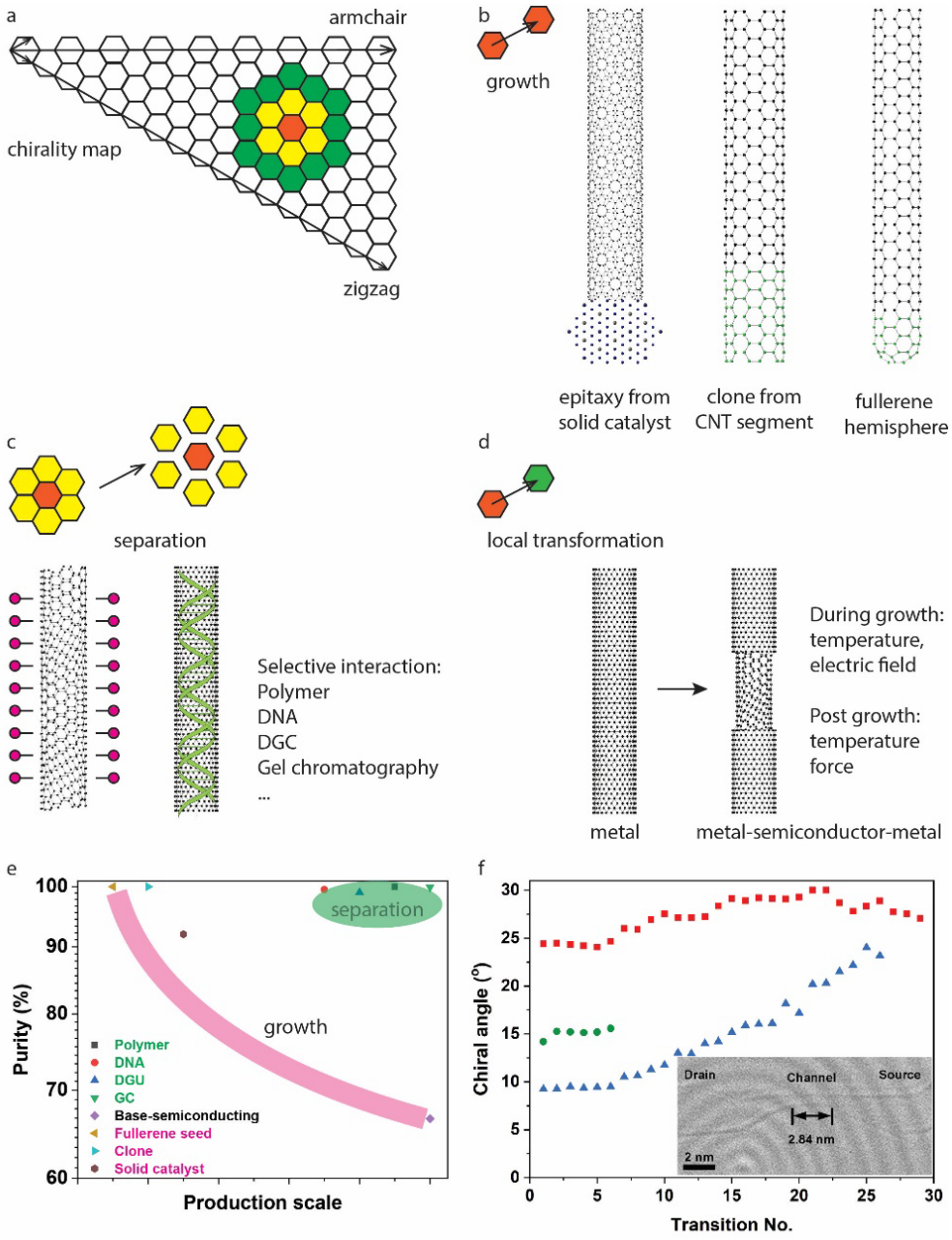

Figure 2. Global and local chirality engineering of carbon nanotubes. (a) Chirality map and schematic distribution around the chirality marked in red. (b) Chirality-controlled growth from solid catalyst, CNT segments and fullerene hemisphere seeds. (c) Chirality separation by selective interaction and dispersion with polymer, DNA, and gel. (d) Local chirality transformation during growth and post-growth process. (e) Plot of the purity against the production scale for global chirality engineering including the growth (pink) and separation (green) approaches. (f) An example of the local chirality transformation following an increasing chiral angle trend to produce a ~2.8 nm long CNT transistor, shown in the insert[102].

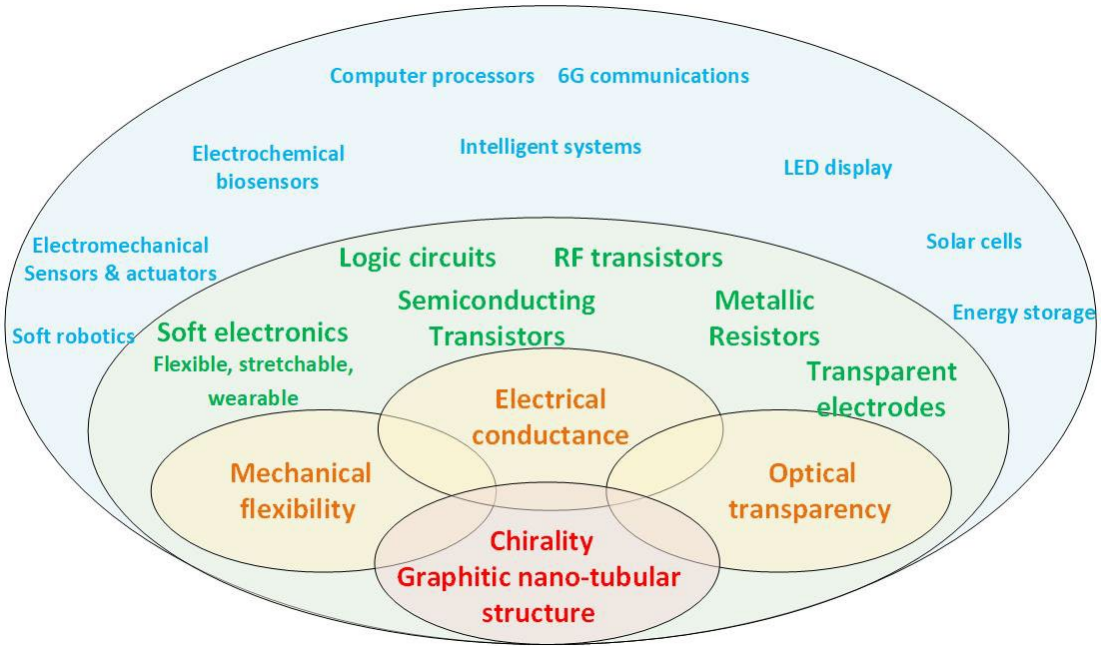

Figure 3. Progresses of CNT electronic devices based on the chirality. Fundamentally, the electronic properties of CNTs are determined by the chirality. In addition, the functions of CNT electronic devices are also dependent on the physical and chemical properties, such as the mechanical flexibility and optical transparency. With the resistors (a) and transistors (b) as the building blocks, complex CNT electronic devices have been developed, ranging from (c) extremely scaled field effect nanotransistors with the gate length of 5 nm[7], (d) modern microprocessors for computers[10], (e) radio frequency amplifier for wireless communications[11], (f) transparent electrodes for organic light-emitting diodes (OLEDs)[12], (g) flexible and transparent transistors on polymer substrates[124], (h) pressure sensor based-electronic skin[145].

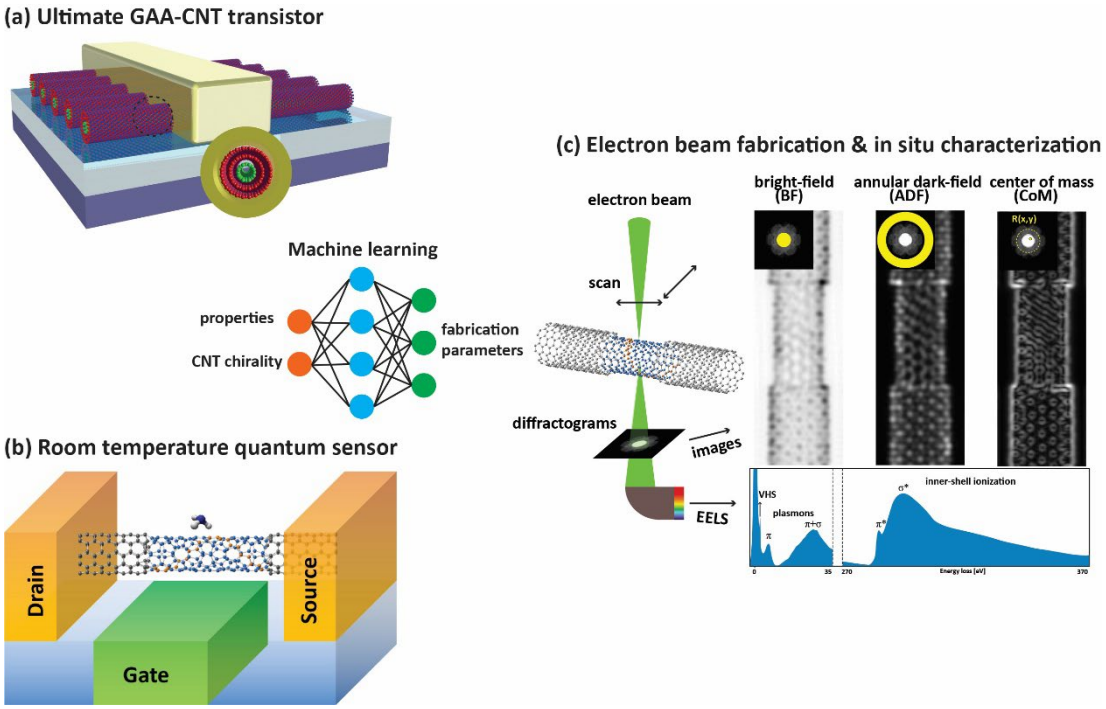

Figure 4. Perspective on chirality-engineered CNT electronics. (a) Ultimate CNT transistors with van der Waals gate-all-around configuration. (b) Ultra-short CNT molecular junction transistors for room temperature quantum sensor of individual gas molecules. (c) Fabrication of CNT junction devices by focused electron beam and in situ characterization by advanced 4D-STEM.

Short summary

Chirality fundamentally determines the electrical properties of CNTs. Here we summarize the approaches in controlling the global chirality distribution and local chirality junctions. After reviewing the progress in CNT electronic devices, a perspective on the CNT quantum devices is presented.